Summer 2022

Novel Synthetic Strategies Toward Polyolefin-Grafted Nanoparticles

Richard Tran Ly

NOVEL SYNTHETIC STRATEGIES TOWARD POLYOLEFIN-GRAFTED NANOPARTICLES

by

Richard Tran Ly

Bachelor of Science
University of Central Florida, 2017

Submitted in Partial Fulfillment of the Requirements

For the Degree of Doctor of Philosophy in

Chemistry

College of Arts and Sciences

University of South Carolina

2022

Accepted by:

Brian Benicewicz, Major Professor

Chuanbing Tang, Committee Member

Aaron Vannucci, Committee Member

Monirosadat Sadati, Committee Member

Cheryl L. Addy, Interim Vice Provost and Dean of the Graduate School

DEDICATION

To my parents.

Thank you for all you've done to give us a better opportunity.

ACKNOWLEDGEMENTS

I owe a great deal of gratitude to my advisor, Prof. Brian Benicewicz. During my time here, he's been an amazing mentor and supporter. He's shown the importance of loving what he does by his excitement in scientific conversations and expresses a genuine interest in helping find one's passion.

Thank you to my committee members, Prof. Chuanbing Tang, Prof. Hans-Conrad zur Loye, Prof. Monirosadat Sadati, and Prof. Aaron Vannucci for their guidance, constructive criticism, and question-filled seminars throughout my doctoral work.

Special thanks to my collaborators at University of Vermont, Prof. Linda Schadler, Dr. Kamlesh Bornani, and Dr. Xin Ning; also Prof. Sanat Kumar, Dr. Mayank Jhalaria, Dr. Sebastian Russel, and Beatrice Bellini at Columbia University. These collaborations have taught me the strengths of interdisciplinary teamwork. Thanks to Prof. Natalia Shustova for the opportunity to work with her group.

During my four years here, I've met a plethora of amazing people, many of whom started as lab mates and fellow colleagues entering graduate school the same year, and are now truly great friends. Thank you to my roommate for all of

graduate school (somehow) and colleague, Eric Ruzicka, for challenging me with synthetic questions and patience. To Caroline Rolhfing and Dr. Ben (Bennie) Howard, thank you for keeping me sane through the tougher days. Thank you to Dr. Laura Murdock for being such a great senior group member and trusting me with the responsibilities of keeping the labs running. Thank you to Prof. Julia Pribyl Ham for all of the Zoom calls to help through the weekly dilemma despite having your own group. I am grateful to Dr. Tianyu Zhu, an incredible synthetic chemist. His patience for the never-ending questions I brought to him is the only thing that could surpass his skills in the lab. Thank you to Dr. Allison Rice and Dr. Gabrielle (Gaby) Leith Small for all the tea over tea. Thank you also to the other previous Benicewicz group members, the Tang group, and the Stefik group. Thanks to the one that had a large role in me joining the Benicewicz group, Miss Susan Hipp.

Finally, special thanks and gratitude to my three brothers: Paul, John, and Victor. I couldn't have done any of this without you guys.

ABSTRACT

Surface functionalization of nanoparticles has proven to be a powerful and versatile strategy in the development of various materials with advanced properties. Polymer brush composition can range from complex copolymers to more simplistic polyolefin, and by functionalizing nanoparticle surfaces, mobility of distinct particles can then be tuned and, therefore, control over dispersion in a polymer matrix can be achieved. Presented in this dissertation are new synthetic strategies for the preparation of polymer nanocomposites.

The first chapter covers a novel synthetic strategy for ethylene/propylene-like copolymers grafted to silica nanoparticles. This approach utilizes Reversible Addition-Fragmentation Chain Transfer (RAFT) polymerization to promote *living polymerization* characteristics with the monomers: isoprene and 2,3-dimethyl-1,3-butadiene (DMB) to obtain an unsaturated precursor which can then be hydrogenated giving the desired ethylene/propylene copolymer nanocomposites. Having the unsaturated precursor is advantageous as it offers facile determination of monomer composition and higher molecular weights can be achieved.

The next chapter discusses a new approach toward polyethylene grafted silica nanoparticles *via* RAFT polymerization with use of the monomer, 1,3-

butadiene followed by mild hydrogenation. Compared to using Ring-opening Metathesis Polymerization (ROMP) approach, this strategy offers an accurate determination of graft density prior to polymerization through monitoring the absorbance of the RAFT agent.

The final chapter is an extension of the previous work in synthesis of ethylene/propylene copolymer nanocomposites. With the incorporation of 1,3-butadiene in the copolymerization, high ethylene content can be achieved. Additionally, previous work has shown sterically hindered butadiene-based monomers, i.e. DMB and isoprene, are less favorable toward complete hydrogenation leaving reactive double bonds in the polymers. Through a thermally-activated thiol-ene click reaction, these double bonds can be consumed and converted into thiol ethers.

The dissertation will conclude with a summary including key points of significant results and main takeaways. Potential direction for future work will also be discussed.

TABLE OF CONTENTS

LIST OF TABLES

LIST OF FIGURES

LIST OF SCHEMES

LIST OF ABBREVIATIONS

ATRP ..... atom transfer radical polymerization

BD 1,3-butadiene

CRP ..... controlled radical polymerization

CTA ..... chain transfer agent

DCC ..... N,N′-dicyclohexylcarbodiimide

DCP ..... dicumyl peroxide

DLS ..... dynamic light scattering

DMAP 4-dimethylaminopyridine

DMB 2,3-dimethyl-1,3-butadiene

DoPAT ..... 2-(((dodecylthio)carbonothioyl)thio)propanoic Acid

DSC ..... differential scanning calorimetry

EPR ..... ethylene-propylene copolymer

FTIR ..... Fourier-transform infrared spectroscopy

GPC ..... gel-permeation chromatography

HDPE ..... high-density polyethylene

*i*PP ..... isotactic polypropylene

ITO ..... indium tin oxide

LDPE ..... low-density polyethylene

LLDPE ..... linear low-density polyethylene

NMP ..... nitroxide-mediated polymerization

NMR ..... nuclear magnetic resonance

PBD ..... polybutadiene

PDMB ..... poly(2,3-dimethyl-1,3-butadiene)

PIP ..... polyisoprene

PNC ..... polymer nanocomposites

RAFT ..... reversible addition-fragmentation chain transfer

ROMP ..... ring-opening metathesis polymerization

ROP ..... ring opening polymerization

SEM ..... scanning electron microscopy

SI-CRP ..... surface-initiated controlled radical polymerization

SI-RAFT ..... surface-initiated reversible addition-fragmentation chain transfer

SI-ROMP ..... surface-initiated ring-opening metathesis polymerization

TEMPO ..... (2,2,6,6-tetramethylpiperidin-1-yl)oxidanyl

TGA ..... thermogravimetric analysis

THF ..... tetrahydrofuran

TSH ..... para-toluenesulfonyl hydrazide

UV-Vis ..... ultraviolet-visible spectroscopy

CHAPTER 1

INTRODUCTION

1.1 Polymer Brushes

Surface functionalization with polymers has become an effective strategy toward building materials with different properties for various applications such as bacterial coatings,[1] gas separation,[2] and mechanical reinforcements.[3] With the advancements of synthetic strategies, the scope of potential polymer architectures has expanded immensely which can be seen with diverse polymer brush compositions without sacrificing control over the complex nature of the architecture. Controlled radical polymerization (CRP) techniques such as reversible addition-fragmentation chain transfer (RAFT), atom transfer radical polymerization (ATRP), and nitroxide-mediated polymerization (NMP) are effective methods for controlled polymer synthesis. Other routes such as ring-opening metathesis polymerization (ROMP) and ring opening polymerization (ROP) are also effective routes, where the driving force for polymerization is relief of ring strain.

The most general way to describe a polymer brush would be thin polymer films where each individual polymer chain is attached directly to the surface. Two important variables of the grafted polymer layer are chain length and graft density (chains per unit area), which lead to a spectrum of chain conformations and ultimately control the properties of the polymer brush. At lower densities, the polymers will simply collapse onto themselves giving a "mushroom" or

"pancake" appearance, and as the graft density increases, the closer polymer neighbors end up pushing each other up away from the surface giving a more "brush" appearance (Figure 1.1). Despite the clear differences in each conformation, the term "brush" is typically used to describe all attached polymers, regardless of conformation.

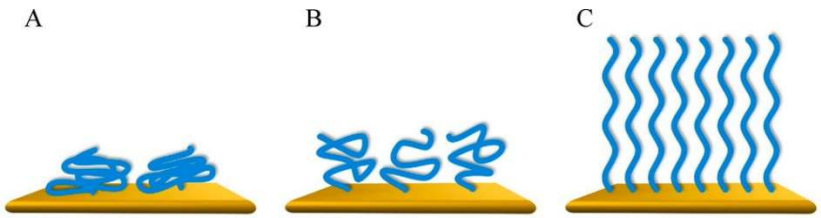

Figure 1.1: Illustration of different surface-attached polymer conformations: (A) pancake, (B) mushroom, and (C) brush. (reprint from ref [4], not subject to US copyright)

One important aspect focused on when building macromolecules with polymer brushes is how the polymers are attached. There are several approaches that are observed with two common ones being *grafting to* and *grafting from*. These are favorable as the polymers are covalently bound to the surface thus mitigating polymers being easily removed, more typical in physisorption. In *grafting to*, the polymers are first synthesized and capped with an end group that can readily react with the surface. By synthesizing the polymers first, purification to obtain a desired molecular weight can be done so there is more control to have more uniformity in molecular weight amongst the brushes. The downside to this approach, however, is that it's limited by lower graft densities; once one polymer

is tethered to the surface, the polymer could collapse onto itself, thus shielding the surface and lowering the chance of attaching an additional polymer (Figure 1.2A). Higher graft densities can be achieved more easily by following a *grafting from* approach. Through this route, the surface is functionalized with a species, such as initiator or iniferter, [5] where polymerization can occur and as the polymerization occurs, the unattached polymer end grows further away from the surface, forming the brush (Figure 1.2B). By having each polymer grow from the surface, a higher density can be achieved, but there is less control over each polymer molecular weight. This can be alleviated by using the controlled polymerization techniques mentioned previously.

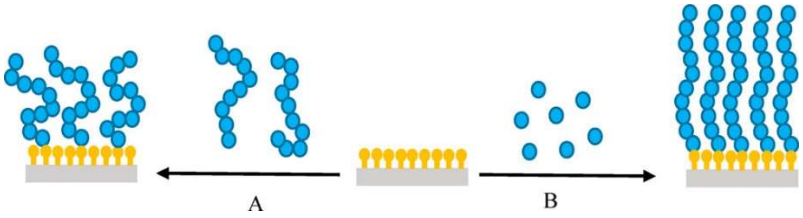

Figure 1.2: Illustration of different approaches to tether polymers to a surface: (A) grafting to and (B) grafting from (Reprint from ref [4], not subject to US copyright)

Polymerization reactions have come a long way, from once being described as "a sloppy affair" to now having control and precision similar to that of natural product synthesis.[6] One major advancement in polymer chemistry was the development of living polymerization, where rate of initiation is significantly higher than rate of propagation. This would cause all active species to form simultaneously and chain growth to occur at the same rate until all monomer is

consumed, resulting in polymers with predictable molecular weights and low Dispersity (Đ, uniformity of polymer molecular weight). This was first described in 1956 by Michael Szwarc through living anionic polymerization of styrene with use of an alkali metal and naphthalene in tetrahydrofuran. While living radical polymerization was first demonstrated in 1982 by Otsu et al.,[7] it wasn't until the mid-1990s that living radical polymerization gained widespread interest in the field through several major contributors: Georges et al. by polymerizing styrene with NMP,[8] Rizzardo, Moad, and Thang, with their work toward developing RAFT polymerization,[9] and Matyjaszewski et al. with their work toward ATRP.[10] To benefit from these desirable results, CRP techniques were applied toward synthesis of polymer brushes in an approach known as surface-initiated polymerization, and while TEMPO and ATRP are effective in giving well-controlled polymerizations, RAFT polymerization is advantageous as it can work at low temperatures and avoids transition metal catalysts.

1.2 Polymer Nanocomposites

Polymer nanocomposites (PNCs) are a class of hybrid materials composed of both a nano-sized filler and a polymer matrix, and were first studied in the 1940s with the intent on improving materials used for tires.[11] It wasn't until the 1990's, however, when Toyota Central Research discovered incorporation of platelet-like clay nanoparticles into a polymeric system would yield a product with

significantly higher mechanical and thermal properties.[12] Afterwards, the field of PNCs grew immensely, using various organic polymer matrices with a myriad of inorganic fillers such as spherical nanoparticles (e.g. silica, titania),[13] carbon nanotubes,[14] metal nanowires,[15] and quantum dots. The main benefit of PNCs is the ability to tune the properties toward a specific application (Figure 1.3). In the design of a polymer nanocomposite, the inorganic filler offers functionality, meaning the initial properties are transferred to the hybrid material. So gold nanoparticles would be used for optical applications[16] or ITO for conductive applications.[17] Silica nanoparticles are an attractive choice as they can be tuned towards both optical and electrical applications, but also have impressive mechanical and thermal properties.[18] Aside from the type of compound used as the filler, size of the particles also has a large effect on overall properties; while "nano" in "nanoparticle" refers to a material sized between 1 to 100 nm, the change in size simply from a 10 nm particle to 20 nm will result in the surface area to be four times as much for the 20 nm particle. With the significant increase in surface area, the importance of the particle interface is stressed. This is known as the PNC "effect". An important note here is while higher or lower size will drastically change the surface area, maximizing surface area does not necessarily improve the interfacial interactions as the change in surface area will affect the properties differently, for example, in conductivity versus permeability.[20,21] The surface to

volume ratio increases exponentially as the diameter of the particle decreases, so small amounts or volumes of nanoparticles can provide large amounts of surface area.

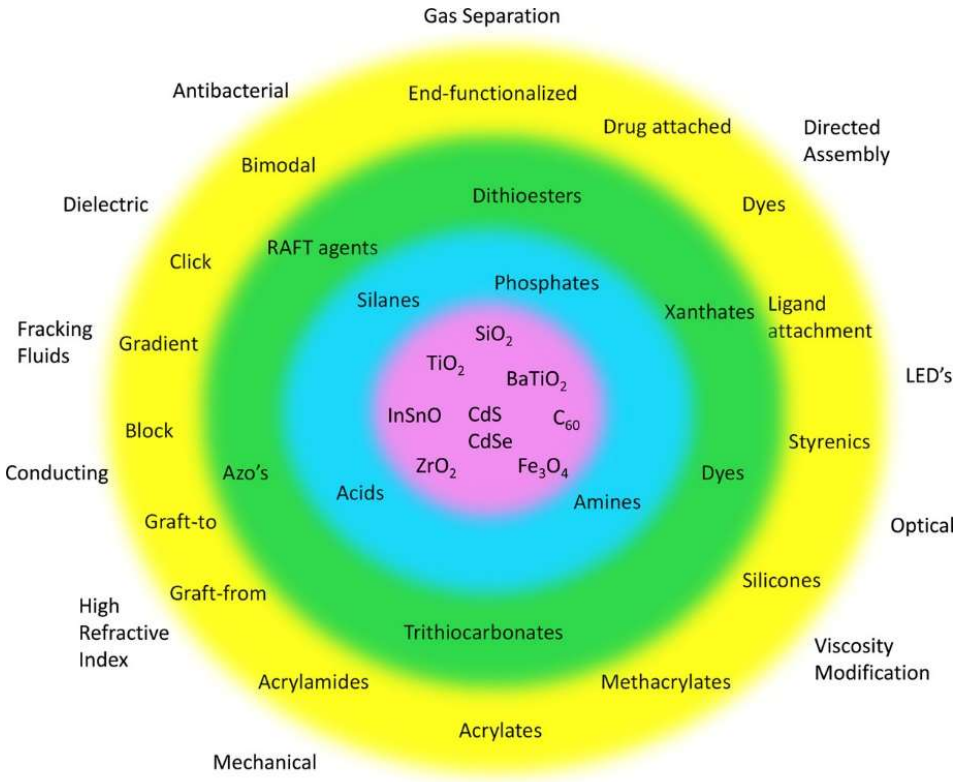

Figure 1.3: Schematic showing the wide range of variability of nanocomposite materials, with different types of nanoparticles, surface functionality, and applications they can be optimized toward. Reproduced with permission from ref [19].

While the choice of nanoparticles has a large role in the overall properties of the hybrid product, the polymer component is equally important. Generally, polymers are typically processable and have superior mechanical properties to that of small molecules. In addition, polymer design has a direct effect on properties and can result in a myriad of different characteristics. So, combining

these two classes of materials can potentially give a hybrid material with the key benefits of each individual component. However, it's important to note that simply mixing nanoparticles and a polymer matrix will not guarantee the desired properties will be obtained. This is due to the incompatibility of the components; inorganic nanoparticles are typically extremely hydrophilic and organic polymer matrices are hydrophobic. This means blending of the two materials will more than likely lead to aggregation of the particles. One powerful strategy to mitigate this issue is through grafting polymers directly onto the particles, resulting in the particle interface to be more compatible with the polymer matrix (Figure 1.4).[22, 23]

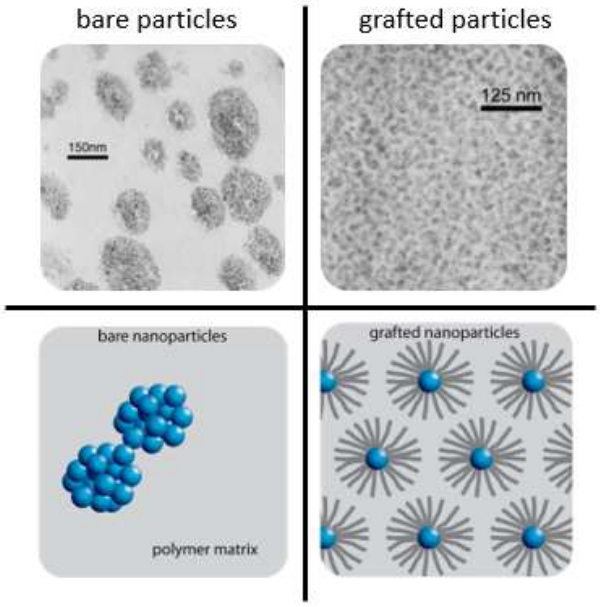

Figure 1.4: SEM imaging and illustration of bare particles aggregated in a polymer matrix (left) and well-dispersed grafted particles (right).

1.3 Olefin Polymers

Polyolefin materials, specifically polyethylene and polypropylene, account for over 2/3rds of commodity plastics, annually producing more than 70 and 50 million metric tons, respectively.[24] Ethylene polymers (high-density polyethylene (HDPE), low-density polyethylene (LDPE), and linear low-density polyethylene (LLDPE)) are popular plastics as they offer high chemical inertness and strength with low density. Isotactic polypropylene (*i*PP) offers ease of processing, low cost of production, and good mechanical properties but, unlike polyethylene, lacks in ductility and toughness.[25, 26]

Because of advancements in production, the amount of plastics being produced is growing exponentially while the percentage being recycled struggles to keep up; in 2018, only 8.7% of plastics were recycled.[27] Due to this quickly growing problem, countless approaches have and are being explored to alleviate the issue such as sustainable plastics,[28] biodegradable plastics,[29] polyethylene-mimics,[30] or upcycling (e.g. plastics converted to wax for production of asphalt).[31] While these have some promise of lessening the amount plastics being thrown out and accumulating in the environment, the cost of essentially trying to replace mass produced plastics, such as polyethylene, is extremely undesirable from a financial aspect.

Recycling is a common approach toward reducing plastic waste; however, a key factor affecting the recyclability is the incompatible nature of many polymer mixes resulting in poor mechanical properties, inferior chemical and thermal stability, and aging behavior compared to the original constituents.[32] This observation is exemplified in the blending of PE and PP; despite their similar structures, this pair of polyolefins are immiscible resulting in phase separation. Individually, the strain at break point for PE and *i*PP are 300% and 800%, respectively, but once blended, it drops down to a mere 12%. So, promoting a homogeneous mixture would afford a blended material with practical properties. An effective approach to improve miscibility is with use of a compatibilizer. Compatibilizers are additives that work by lowering surface tension and promoting interfacial adhesion between the two polymers and are typically designed with structural similarities to the original constituents[33-35] (Figure 1.5). With that in mind, a copolymer containing both ethylene and propylene units would have the potential to act as a compatibilizer for an PE/PP mixture.

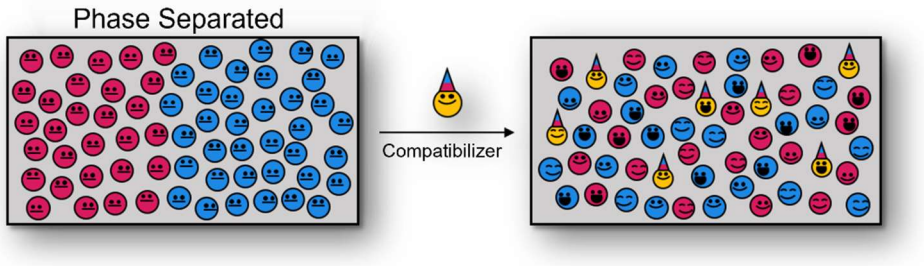

Figure 1.5: Cartoon depiction of compatibilizer added to phase separated mixture to afford homogenous mixture.

Individually, commercial polyethylene and polypropylene are synthesized using Ziegler-Natta catalysts with ethylene or propylene gas.[36-38] This chain growth polymerization uses a transition metal catalyst (typically titanium or zirconium) in conjunction with an organoaluminum cocatalyst (such as triethylaluminum). The accepted mechanism has the alkyl group coordinate to the metal center through an olefin insertion. Once coordinated, a rearrangement occurs, and the olefin is added to the growing polymer chain. This polymerization technique typically yields a polymer with broad dispersity, but can also lead to well-controlled stereochemistry (e.g., *i*PP).[39]

Following a similar synthetic approach for an ethylene/propylene copolymer, Eagen et al.[40] used a pyridylamidohafnium catalyst. In this work, the chain was grown first with ethylene then with propylene, yielding a block copolymer (Figure 1.6). Compared to Ziegler-Natta, this approach afforded higher molecular weight polymers without elevated dispersities (1.3–1.4). Additionally,

a 5% incorporation of the copolymer to a PE/PP blend improved the strain at breakpoint from 12% to 600% demonstrating its effectiveness in improving interfacial adhesion. The downside to this approach, however, is the limitation of block copolymers; the only way to determine polymer composition is through using high temperature (~115 °C) gel-permeation chromatography (GPC) as more common techniques (e.g. NMR) could not distinguish between the similar structures of ethylene and propylene units. Also, it was shown due to the high crystallinity of the block copolymer that precipitation during polymerization was an issue, leading to broad molecular weight distributions.

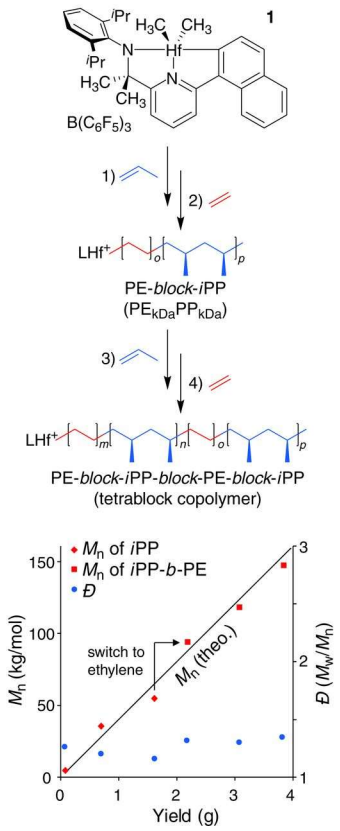

Figure 1.6: Ethylene/Propylene block copolymers synthesized using isoselective pyridylamidohafnium catalyst. From ref [40]. Reprinted with permission from AAAS.

An alternative approach toward incorporating the different olefin units was done by Klimovica et al.[41] In this work, they developed a copolymer with a polyethylene backbone and incorporated the propylene units using a grafting through approach; the propylene units were first synthesized into a macromonomer terminated with an allyl group. Copolymerization was then performed with the macromonomer and ethylene gas. In doing so, crystallinity of the copolymer was diminished greatly due to the propylene macromonomer side chain disrupting chain packing. This approach proved effective as 5% addition to

a PE/PP blend would improve the break point to 950%. Although impressive, this number could likely be improved with a sample of higher purity; during copolymerization, the reaction was terminated prior to complete consumption of the macromonomer to avoid a polypropylene-rich tail, and as a result, the system contained up to 40% unreacted macromonomer. So, challenges in purification can be attributed to incorporation of propylene through use of the macromonomer. Additionally, extremely high dispersities (~20) showed low degree of control in the propylene incorporation while only reaching a maximum molecular weight of 28 kDa.

In the previously discussed works, designing a copolymer with ethylene and propylene units displayed excellent potential as a compatibilizer in PE/PP blends. The issue, however, lies in characterization of the semi-crystalline polymers; low solubility poses an issue, even with the "polypropylene" side chains. In addition to high temperatures, niche instrumentation using toxic chemicals (e.g. chlorinated benzenes) are required for determination of molecular weight and polymer composition. If a soluble polymer intermediate could be created, characterization could be performed with more common techniques. Recent work by Frech et al.[42] discuss an approach toward an ethylene-free synthesis of polyethylene copolymers utilizing post-polymerization modification. In this approach, polymerization is performed with a phthalimide ester monomer

(Figure 1.7), and is then followed by a photochemically or thermally induced decarboxylation resulting in a PE backbone. As stated earlier, solubility is the challenge. The work here only goes over decarboxylation of copolymers as the other units promote solubility. If decarboxylation were to occur on a homopolymer of the phthalimide ester (Figure 1.7A), the polymer would precipitate before complete conversion. So, while an effective route toward ethylene/ester copolymers, this route would not be effective toward the desired ethylene/propylene copolymer.

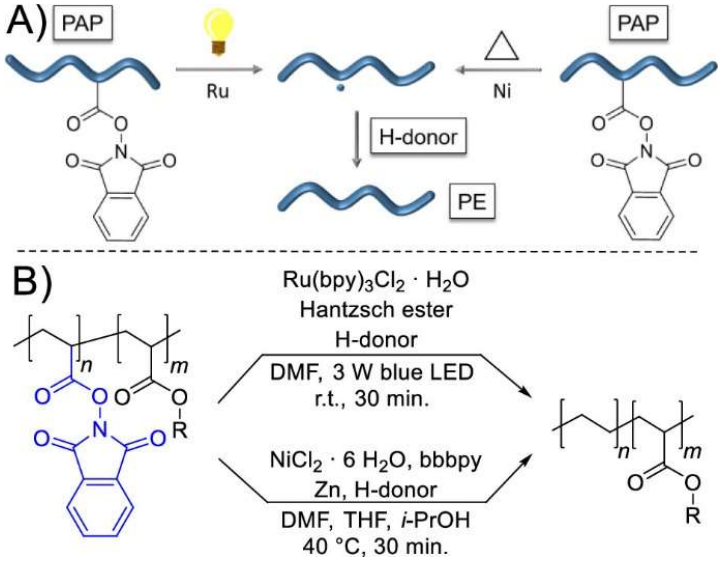

Figure 1.7: (A) General reaction pathways for photochemically and thermally induced decarboxylation of poly[N-(acryloyloxy)phthalimide] (PAP) and (B) Detailed reaction parameters for decarboxylation of copolymers. Reproduced with permission from ref [42].

1.4 Dissertation Outline

The work in this dissertation focuses on design, synthesis, and characterization of novel strategies toward grafted polyolefin brushes onto

nanoparticles. The principles discussed in chapter 1 were necessary in designing the experimental approach toward synthesis of the polyolefin brushes in Chapters 2-4.

Chapter 2 focuses on the copolymerization of butadiene monomer derivatives (i.e. isoprene and 2,3-dimethyl-1,3-butadiene, or DMB) to afford an unsaturated precursor to the desired ethylene/propylene copolymer. A set of experiments were performed varying the feed input of isoprene to DMB. The polymer composition was measured using ^{1}H NMR spectroscopy. Utilizing SI-RAFT polymerization resulted in controlled polymerization from the nanoparticle surfaces. Following the reduction of the double bonds using para-toluenesulfonyl hydrazide (TSH) as the hydrogen source, ethylene/propylene copolymers were obtained. Thermal analysis was performed to monitor changes before and after hydrogenation.

Chapter 3 explores another direction utilizing strategies from Chapter 2 toward designing a new approach for an ethylene-free synthesis of polyethylene-grafted nanoparticles via RAFT Polymerization. Much nanocomposite work in the Benicewicz group revolves around the use of SI-RAFT polymerization as it offers excellent control over dispersity and molecular weight. Additionally, RAFT agents tethered to a nanoparticle surface can easily be quantified simply by ultraviolet-visible spectroscopy (UV-Vis) allowing for an alternative approach toward

molecular weight determination. It also offers the benefit of knowing graft density prior to polymerization. Due to the synthetic challenges of synthesizing polyethylene nanocomposites, there are few literature examples present. In this work, we present an approach toward polyethylene-grafted nanoparticles via SI-RAFT polymerization with 1,3-butadiene (BD). Synthesis, characterization, and challenges are discussed.

Chapter 4 is focused on solving an inherent problem of synthesizing ethylene/propylene graft polymers with high ethylene content. In Chapter 2, the minimum ethylene to propylene percentage possible was 50% through hydrogenation of pure polyisoprene. In many practical applications, the lower range of 0 to 49% would need to be explored. Copolymerization of isoprene and (BD) could afford this range and were investigated in this chapter. Additionally, an alternative approach toward controlled conversion of residual double bonds was explored utilizing thiol-ene click chemistry.

1.5 References

1. Ohm, C.; Welch, M. E.; Ober, C. K. Materials for Biosurfaces. *J. Mater. Chem.* **2012**, *22* (37), 19343.

2. Baker, R. W. Gas Separation. *Membrane Technology and Applications*, 2nd ed.; John Wiley & Sons: New York, **2004**; pp 301-351.

3. Chen, Q.; Gong, S.; Moll, J.; Zhao, D.; Kumar, S. K.; Colby, R. H. Mechanical Reinforcement of Polymer Nanocomposites from Percolation of a Nanoparticle Network. *ACS Macro Lett.* **2015**, *4* (4), 398-402.

4. Zoppe, J. O.; Atama, N. C.; Mocny, P.; Wang, J.; Moraes, J.; Klok, H. Surface-Initiated Controlled Radical Polymerizations: State-of-the-Art, Opportunities, and Challenges in Surface and Interface Engineering with Polymer Brushes. *Chem. Rev.* **2017**, *117* (3), 1105-1318.

5. Otsu, T. Iniferter Concept and Living Radical Polymerization. *J. Polym. Sci. A Polym. Chem.* **2000**, *38* (12), 2121-2136.

6. Grubbs, R. B.; Grubbs, R. H. 50th Anniversary Perspective: Living Polymerization – Emphasizing the Molecule in Macromolecules. *Macromolecules*, **2017**, *50*, 6979-6997.

7. Otsu, T.; Yoshida, M.; Tazaki, T. A Model for Living Radical Polymerization. *Makrol. Chem., Rapid Commun.* **1982**, *3*, 133-140.

8. Georges, M. K.; Veregin, R. P. N.; Kazmaier, P. M.; Hamer, G. K. Narrow Molecular-Weight Resins by a Free-Radical Polymerization Process. *Macromolecules*, **1993**, *26*, 2987-2988.

9. Chiefari, J.; Chong, Y. K.; Ercole, F.; Krstina, J.; Jeffery, J.; Le, T. P. T.; Mayadunne, R. T. A.; Meijs, G. F.; Moad, C. L.; Moad, G.; et al. Living Free-Radical Polymerization by Reversible Addition-Fragmentation Chain Transfer: The RAFT Process. *Macromolecules*, **1998**, *31*, 5559-5562.

10. Wang, J. S.; Matyjaszewski, K. Controlled Living Radical Polymerization – Atom-Transfer Radical Polymerization in the Presence of Transition-Metal Complexes. *J. Am. Chem. Soc.* **1995**, *117*, 5614-5615.

11. Giannelis, E. P.; Krishnamoorti, R.; Manias, E. Polymer-Silicate Nanocomposites: Model systems for Confined Polymers and Polymer Brushes. *Adv. Polym. Sci.* **1999**, *138*, 108-147.

12. Kojima, Y.; Usuki, A.; Kawasumi, M.; Okada, A.;Fukushima, Y.;Kurauchi, T.; Kamigaito, O. Mechanical-Properties of Nylon 6-Clay Hybrid. *J. Mater. Res.* **1993**, *8*, 1185-1189.

13. Tsagaropolous, G.; Eisenburg, A. Dynamic-Mechanical Study of the Factors Affecting the 2 Glass-Transition Behavior of Filled Polymers – Similarities and Differences with Random Ionomers. *Macromolecules* **1995**, *28*, 6067-6077.

14. Moniruzzaman, M.; Winey, K. I. Polymer Nanocomposites Containing Carbon Nanotubes. *Macromolecules* **2006**, *39*, 5194-5205.

15. Rahman, M. T.; Kabir, M. F.; Gurung, A.; Reza, K. M.; Pathak, R.; Ghimire, N.; Baride, A.; Wang, Z.; Kumar, M.; Qiao, Q. Graphene Oxide-silver Nanowire Nanocomposites for Enhanced Sensing of Hg^{2+}. *ACS Appl. Nano Mater.* **2019**, *2*(8), 4842-4851.

16. Jhang, W.; Li, C.; Wang, A.; Lie, C.; Hsu, S. Tunable Optical Properties of Plasmonic-polymer Nanocomposites Comprised of Multilayer Nanocrystal Arrays Stacked in a Homogeneous Polymer Matrix. *ACS Appl. Mater. Interfaces* **2020**, *12*(46), 51873-51884.

17. Gangopadhyay, R.; De, A. Conducting Polymer Nanocomposites: A Brief Overview. *Chem. Mater.* **2000**, *12*(3), 608-622.

18. Ilangovan, S.; Kumaran, S. S.; Vasudevan, A.; Naresh, K. Effect of Silica Nanoparticles on Mechanical and Thermal Properties of Neat Epoxy and Filament Wounded E-glass/epoxy and Basalt/epoxy Composite Tubes. *Mater. Res. Express* **2019**, *6*(8).

19. Kumar, S. K.; Benicewicz, B. C.; Vaia, R. A.; Winey, K. I. 50^{th} Anniversary Perspective: Are Polymer Nanocomposites Practical for Applications? *Macromolecules* **2017**, *50*, 714-731.

20. Akcora, P.; Kumar, S. K.; Moll, J.; Lewis, S.; Schadler, L. S.; Li, Y.; Benicewicz, B. C.; Sandy, A.; Narayananm S.; Ilavsky, J.; Thiyagarajan, P.; Colby, R. H.; Douglas, J. F. "Gel-like" Mechanical Reinforcement in Polymer Nanocomposite Melts. *Macromolecules* **2010**, *43*, 1003-1010.

21. Maillard, D.; Kumar, S. K.; Fragneaud, B.; Kysar, J. W.; Rungta, A.; Benicewicz, B. C.; Deng, H.; Brinson, L. C.; Douglas, J. F.; Mechanical Properties of Thin Glassy Polymer Films Filled with Spherical Polymer-Grafted Nanoparticles. *Nano Lett.* **2012**, *12*, 3909-3914.

22. Bansal, A.; Yang, H.; Benicewicz, B. C.; Kumar, S. K.; Schadler, L. S. Controlling the Thermomechanical Properties of Polymer Nanocomposites by Tailoring the Polymer-particle Interface. *J. of Polym. Sci.: Part B: Polym. Phys.* **2006**, *44*(20), 2944-2950.

23. Mackay, M. E.; Tuteja, A.; Duxbury, P. M.; Hawker, C. J.; Horn, B. V.; Guan, Z.; Chen, G.; Krishnan, R. S. General Strategies for Nanoparticle Dispersion. *Science* 2006, *311*, 1740-1743.

24. Malpass, D. B.; Band, E. I. "Introduction to Polymers of Propylene" in *Introduction to Industrial Polypropylene*: *Properties, Catalysis, Processes*. (Scrivener, 2012). Pp 1-18.

25. Parameswaranpillai, J.; Pulikkalparambil, H.; Sanjay, M. R.; Siengchin, S. Polypropylene/high-density Polyethylene Based Blends and Nanocomposites with Improved Toughness. *Mater. Res. Express* **2019**, *6*.

26. Nowlin, T. E.; Mink, R. I.; Kissin, Y. V.; Supported Magnesium/Titanium-Based Ziegler Catalysts for Production of Polyethylene. In *Handbook of Transition Metal Polymerization Catalysts*, online ed.

27. Plastics information is from the American Chemistry Council, the National Association for PET Container Resources and The Association of Plastic Recyclers.

28. Zhu, J.; Watson, E. W.; Tang, J.; Chen, E. Y.-X. A Synthetic Polymer System with Repeatable Chemical Stability. *Science* **2018**, *360*(6387), 398-403.

29. Ghosh, K.; Jones, B. H. Roadmap to Biodegradable Plastics – Current State and Research Needs. *ACS Sustainable Chem. Eng.* **2021**, *9*(18) 6170-6187.

30. Haider, T.; Shyshov, O.; Suraeva, O.; Lieberwirth, I.; Delius, M. v.; Wurn, F. R. Long-chain Polyorthoesters as Degradable Polyethylene Mimics. *Macromolecules* **2019**, *52*(6), 2411-2420.

31. Ma, Y.; Zhou, H.; Jiang, X.; Polaczyk, P.; Xiao, R.; Zhang, M.; Huang, B. The Utilization of Waste Plastics in Asphalt Pavements: A review. *Elsevier* **2021**, *2*(15).

32. Teh, J. W.; Rudin, A.; Keung J. C. A Review of Polyethylene-propylene Blends and Their Compatibilization. *Advances in Polymer Technology* **1994**, *13*(1), 1-23.

33. Utracki, L. A. *Commercial Polymer Blends*; Chapman and Hall: London, 1998.

34. Gaylord, N. G. Compatibilizing agents: Structure and function in polyblends. *J. of Macromolecular Sci.: Part A – Chem.* **2006**, *26*(8), 1211-1229.

35. Arriola, D. J.; Carnahan, E. M.; Hustad, P. D.; Kuhlman, R. L.; Wenzel, T. T. Catalytic Production of Olefin Block Copolymers via Chain Shuttling Polymerization. *Science* **2006**, *312*, 714-719.

36. Eisch, J. J. Fifty years of Ziegler-Natta Polymerization: From Serendipity to Science. *Organometallics* **2012**, *31*, 4917-4932.

37. Yang, J.; Huang, B.; Fu, Z.; Fan, Z. Ethylene/1-Hexene Copolymerization with Supported Ziegler-Natta Catalysts Prepared by Immobilizing $TiCl_3(OAr)$ onto $MgCl_2$. *J. Appl. Polym. SCi.* **2015**, *132*, 41329.

38. Fu, T.; Liu, Z.; Cheng, R.; He, X.; Tian, Z.; Liu, B.; Ethylene Polymerization over $MgCl_2/SiO_2$ Bi-supported Ziegler-Natta Hybrid Titanium/Vanadium Catalysts. *Macro. Chem. Phys.* **2017**, *218*, 1700027.

39. Bassett, D. C.; Olley, R. H. On the Lamellar Morphology of Isotactic Polypropylene Spherulites. *Polymer* **1984**, *25*, 935-946.

40. Eagan, J. M.; Xu, J.; Girolamo, R. D.; Thurber, C. M.; Macosko, C. W.; LaPointe, A. M.; Bates, F. S.; Coates, G. W. Combining Polyethylene and Polypropylene: Enhanced Performance with PE/iPP multiblock Polymers. *Science* **2017**, *355*, 814-816.

41. Klimovica, K.; Pan, S.; Lin, T.-W.; Peng, X.; Ellison, C. J.; LaPointe, A. M.; Bates, F. S.; Coates, G. W. Compatibilization of iPP/HDPE Blends with PE-g-iPP Graft Copolymers. *ACS Macro Lett.* **2020**, *9*, 1161-1166.

42. Frech, S.; Molle, E.; Butzelaar, A. J.; Theato, P. Ethylene-free Synthesis of Polyethylene Copolymers and Block Copolymers. *Macromolecules*, **2021**, *54*, 9937-9946.

CHAPTER 2

ETHYLENE/PROPYLENE COPOLYMER NANOCOMPOSITES THROUGH RAFT COPOLYMERIZATION OF ISOPRENE AND 2,3-DIMETHYL-1,3-BUTADIENE[1]

[1]Ly, R. T.; and B. C. Benicewicz. To be submitted to *Macromolecules*.

2.1 Abstract

Through the advancements in surface-initiated polymerizations, a library of polymer brush nanocomposites has been established with brush architecture ranging from complex intricacies to more basic polyolefins, such as polyethylene and polypropylene. Despite these developments and the potential applications, few examples are present in the literature effectively synthesizing ethylene-propylene copolymers grafted to nanosilica fillers. Presented here is a synthetic approach toward an ethylene/propylene copolymer grafted to silica nanoparticles with controllable graft density, molecular weight, and monomer composition. Synthesis, characterization, and challenges faced are discussed.

2.2 Introduction

Polyolefin materials, namely polyethylene and polypropylene lead the industry of commercial synthetic plastics, accounting for over 2/3rd of the plastics produced annually. The widespread use of these polymers from packaging and clothing to car parts and components in medical equipment can be attributed to low cost, good mechanical properties, and ease of processing.[1-3] In addition, polyethylene also has superior toughness and ductility compared to polypropylene. To keep up with the growing demand of advanced materials with superior properties, strategies to improve current conventional polymer systems have been explored, such as use of additives.[4-7] One notable example of this is use

of an ethylene-propylene copolymer (EPR) as an additive to improve the mechanical strength of polypropylene resins. In doing so, the impact strength was enhanced by four times relative to the neat matrix.[8] While an impressive improvement, the tradeoff was shown with the decrease in thermal stability. Work by Gao et al.[9] showed dispersion of attapulgite, a natural fibrillary silicate clay mineral into a ternary blend of the EPR and polypropylene yielded the enhanced impact strength while still retaining thermal stability. In turn, yield strength diminished greatly due to incorporation of the particles leading to several hundred nanometer agglomerates in the polypropylene matrix. So, controlling the dispersion of particles in a polymer matrix could then lead toward realization of property enhancement of materials. This degree of control could be achieved with the use of polymer nanocomposites.[10, 11]

Polymer nanocomposites are a class of materials composed of a nano-sized filler and polymer matrix, and have been explored extensively due to the ability to impart functionality of the particle without losing key characteristics of the polymer constituent, i.e. processability.[12-14] A key component to achieve this control is by use of polymer-grafted nanoparticles; by grafting polymers with similar chemistry to the polymer matrix, nanoparticle compatibility in the matrix is greatly improved, thereby lessening particle aggregation.[15, 16] Utilizing this approach, polyethylene/nanoclay composites were prepared via coordination

polymerization, resulting in well-dispersed clay particles in a polyethylene matrix with superior thermal stability compared to neat polyethylene.[17] Silica nanoparticles are an ideal nanofiller for its low cost, thermal stability, and mechanical strength.[18] Also, previous work on surface-initiated controlled radical polymerization (SI-CRP) has shown to be an effective method toward controlling grafted chain molecular weight while independently varying graft density. Zhang et al.[19] effectively grew poly(methyl methacrylate) onto silica nanoparticles by anchoring initiators promoting ATRP from the surface. While effective in promoting controlled polymerization from the surface of a nanoparticle, graft density could only be characterized afterwards by determining the ratio of polymer to particle mass. SI-RAFT has proven a powerful strategy in synthesis of polymer nanocomposites; in addition to also offering controlled polymerization characteristics, the anchored RAFT agents allow for graft density determination prior to polymerization due to the unique UV-Vis absorbance relative to the particle system.[20, 21]

In this work, we present new synthetic approach using SI-RAFT to prepare ethylene/propylene copolymers grafted to silica nanoparticles with independent control over graft density and polymer composition. The synthesis, characterization, and challenges during synthesis will be discussed.

2.3 Experimental

2.3.1 Materials and Instrumentation

Silica nanoparticles (MEK-ST, 30 wt.% in methyl ethyl ketone, diameter (14±4 nm) were donated by Nissan Chemical Corporation. Dry tetrahydrofuran (THF) was obtained from a dry still solvent system and used immediately. All other chemicals were supplied by Thermo Fisher Scientific, Oakwood Chemicals, Alfa Aesar, Acros Organics, Gelest, or Matrix Scientific. All chemicals were used as received unless stated otherwise. Isoprene and DMB were prepared by filtering through a basic alumina column to remove the inhibitor. Thermogravimetric Analysis (TGA) was performed on a Hitachi Instrument STA7200 under nitrogen atmosphere in a platinum pan from 25 to 800 °C at a ramp of 10 °C/min. Differential Scanning Calorimetry (DSC) was performed on a Hitachi Instrument DSC7020 under nitrogen atmosphere at a heating and cooling rate of 10 °C/min. Samples were sealed in aluminum pans for analysis. Two cycles were performed to erase previous thermal history of samples. ^{1}H NMR spectra were obtained from a Bruker Avance III-HD 300 MHz NMR in $CDCl_3$. UV-Vis spectroscopy was performed on a Shimadzu UV-2450 using an excitation wavelength of 360 nm. Scanning range was from 200 to 400 nm. Samples were prepared in THF. Dynamic light scattering (DLS) measurements were run on a Malvern Zetasizer instrument in glass cuvettes at a scattering angle of 90° with THF as the solvent. Fourier-

Transform Infrared Spectroscopy (FTIR) was performed on a Perkin Elmer Spectrum 100 FT-IR Spectrometer equipped with a Universal ATR Sampling Accessory with runs set at 16 scans.

2.3.2 Activation of 2-(((dodecylthio)carbonothioyl)thio)propanoic Acid (DoPAT)

DoPAT (5.00 g, 14.3 mmol), 2-mercaptothiazoline (1.87 g, 15.7 mmol), and N,N′-dicyclohexylcarbodiimide (DCC) (3.53 g, 17.1 mmol) were all combined in a 100 mL round-bottom flask and dissolved in dry THF (60 mL, 0.23 M). The solution was degassed by bubbling N_2 for 15 minutes. The solution was cooled to 0 °C using an ice bath. A solution of 4-dimethylaminopyridine (DMAP) in THF (174 mg in 5 mL, 1.42 mmol) was added to the stirring solution via syringe. The solution was allowed to slowly reach room temperature and stirred for eight hours. The solution was then filtered to remove a salt by-product and the filtrate was collected, then concentrated under reduced pressure. The crude product was purified *via* column chromatography using a 30% ethyl acetate in hexanes solution as the mobile phase. Recrystallization was performed by dissolving the yellow oil in minimal amounts of THF followed by methanol and cooled to 0 °C overnight to yield a yellow precipitate. The yellow solid was collected and dried (4.19 g, 65%) ^{1}H NMR indicates a pure product. T_m = 33.8 °C (DSC). ^{1}H NMR (300 MHz, $CDCl_3$) δ 6.50-6.40 (q, 1H), 4.70-4.60 (m, 1H), 4.53-4.40 (m, 1H), 3.48-3.37 (m, 1H), 3.37-3.20

(m, 1H), 1.71-1.48 (m, 6H), 1.45-0.98 (m, 22H), 0.92-0.79 (t, 3H). ^{1}H NMR, ^{13}C NMR, and DSC curve found in Figure A.1-A.3.

2.3.3 Synthesis of DoPAT-*g*-SiO_2

A solution (20 g) of colloidal silica particles (30 wt% in methyl ethyl ketone) was added to a 100 mL round-bottom flask equipped with a stir bar and diluted with dry THF (20 mL). To the solution, (3-aminopropyl)dimethylethoxysilane, or aminosilane (375 μL, 1.99 μmol) and n-octyldimethylmethoxysilane, or octylsilane (160 μL, 0.643 μmol). The flask was capped with a rubber septum and secured with copper wire and the solution was degassed by bubbling argon for 15 minutes. The flask was then placed in an oil bath set at 70 °C and reacted for six hours. The solution was cooled to room temperature and the nanoparticles were precipitated from solution by the addition of hexanes followed by centrifugation of solution at 6,500 rpm for five minutes. The supernatant was discarded and the solids were re-dispersed in THF (20 mL). Activated DoPAT (180 mg, 0.40 mmol) was added and the solution was stirred for eight hours without presence of light. Afterwards, the nanoparticles were precipitated with the addition of methanol and centrifugation at 6,500 rpm for five minutes. The nanoparticles were re-dispersed in THF and this was repeated until the supernatant no longer had any color. The particles were dried overnight to yield large yellow solids. The particles were stored at -25 °C for

further use. UV-Vis was taken to determine graft density by observing the absorbance at 309 nm.

2.3.4 General Procedure for Free Polymerization of 2,3-dimethyl-1,3-butadiene (DMB) and Isoprene with RAFT

To a 50 mL metal reactor, DoPAT (25 mg, 0.0713 mmol), a solution of dicumyl peroxide, or DCP in toluene (0.01 M, 1.07 mL), and a combination of isoprene and DMB were added. The species of the reaction were held at a ratio of 2,500:1.0:0.15 with [monomer]:[CTA]:[initiator] where [monomer] is the combined ratio between the isoprene and DMB. The metal reactor was placed in an oven equipped with a rotating apparatus and set at 150 °C for three days. The solution was allowed to cool to room temperature and the resulting polymer was collected by addition of methanol followed by centrifugation at 6,500 rpm for five minutes. The solids were re-dispersed in THF and this was repeated three times to remove impurities. The product was dried under reduced pressure and the polymer composition was determined using ^{1}H NMR.

2.3.5 General procedure for SI-RAFT Copolymerization of 2,3-dimethyl-1,3-butadiene (DMB) and Isoprene

In a typical polymerization, DoPAT-*g*-SiO_2 (100 mg) with a graft density of 53.9 μmol/g was dissolved in dry THF (5.0 mL). A solution of DCP (0.01 M, 800 μL) with a combination of isoprene and DMB depending on the desired

ethylene:propylene ratio was added. The species of the reaction were held at a ratio of 2,500:1:0.15 with [monomer]:[CTA]:[initiator] where [monomer] is the combined ratio between the isoprene and DMB. The solution was decanted into metal reactors and rotated in an oven set at 115 °C for four days. The solution was allowed to cool to room temperature and the resulting polymer grafted nanoparticles were collected by addition of methanol followed by centrifugation at 6,500 rpm for five minutes. The solids were re-dispersed in THF and this was repeated three times to remove free polymer. The product was dried under reduced pressure and molecular weight was determined via TGA and polymer composition was determined using ^{1}H NMR.

2.3.6 General Hydrogenation Reaction

In a typical reaction, the unsaturated copolymer nanocomposite (1,500 mg, 22.46 mmol in respect to double bonds) and *o*-xylene (150 mL) were added to a round-bottom flask and dissolved at 90 °C. After a clear solution was observed, *para*-toluenesulfonyl hydrazide, or TSH (12.6 g, 67.38 mmol), and tri-n-propyl amine, or Pr_3N (12.4 mL, 67.38 mmol) were added. A condenser was attached and the solution was heated to 145 °C for three hours. The solution was then cooled to room temperature and the solution was decanted into methanol to yield a cloudy suspension. Centrifugation at 6,500 rpm for five minutes was performed to yield

a yellow gel. Remaining solvents were removed under vacuum to yield a transparent gel. ^{1}H was performed to determine degree of hydrogenation.

2.4 Results and Discussion

A synthetic strategy was developed toward controlled synthesis of an ethylene/propylene copolymer grafted to silica nanoparticles detailed in Scheme 2.1. To begin, silica nanoparticles were functionalized with an aminosilane reagent at varying feed ratio along with an alkylsilane reagent to cap any unreacted silanol groups. The amine-functionalized nanoparticles were then reacted with an activated RAFT agent, DoPAT, to attach RAFT agents directly onto the surface. RAFT activation requires a DCC coupling reaction to promote reactivity of the carbonyl carbon over reaction with the trithioester. Varying the feed ratio of the aminosilane reagent allowed for tuning the graft density of particles prior to polymerization. After purification from unreacted RAFT agents, the DoPAT-functionalized nanoparticles were then reacted with the monomers, isoprene (IP) and 2,3-dimethyl-1,3-butadiene (DMB) to yield the unsaturated precursor. After a mild hydrogenation reaction[22] using para-toluenesulfonyl hydrazide, or TSH as the reducing agent, the unsaturated polymer was converted to the desired saturated copolymer composed of ethylene and propylene units. It is important to note that the use of DMB inherently introduces a head-to-head propylene isomeric

structure into the copolymers. A library of samples was prepared through this approach. Characterization data is shown in Table 2.1.

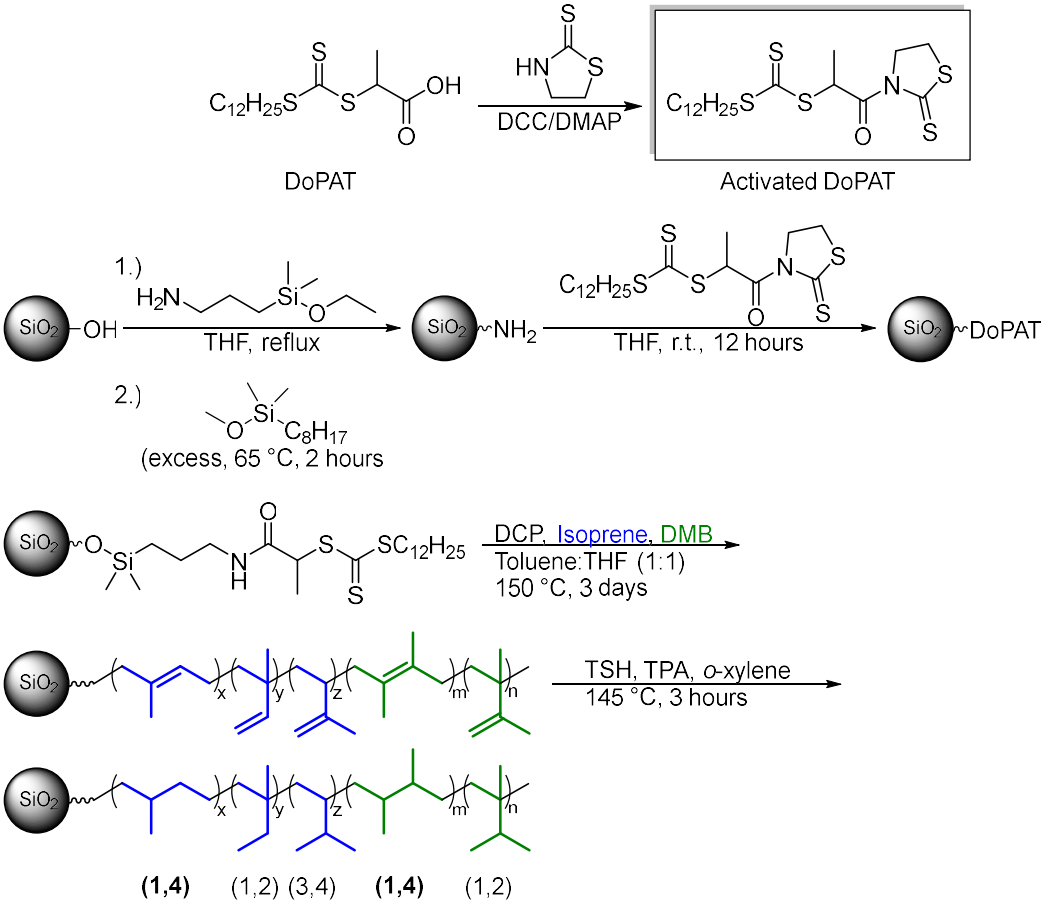

Scheme 2.1 Synthetic approach toward ethylene/propylene copolymers grafted to silica nanoparticles

Table 2.1: Reaction conditions and results of isoprene and DMB copolymerization

Entry	Aminosilane Feed (μL)[a]	Graft Density (ch/nm^2)[b]	Molecular Weight (kDa)[c]	Isoprene Percentage[d]
1	25	0.060	98.1	20/13
2	25	0.060	65.9	50/35
3	25	0.060	47.9	80/56
4	100	0.213	59.2	20/27
5	100	0.213	67.8	50/39
6	100	0.213	48.4	80/75
7	150	0.318	87.2	20/28
8	150	0.318	76.1	50/40
9	150	0.318	67.1	80/71

Polymerizations were all performed at a ratio [Monomer]:[CTA]:[Initiator] of 2,500:1.0:0.15. [a]Feed ratio of aminosilane per 10 g of SiO_2 nanoparticles. [b]Graft density was determined prior to polymerization *via* UV-Vis. [c]Molecular weight was determined *via* TGA. [d]Isoprene percentage in DMB was expressed as theoretical/experimental where experimental was determined via ^{1}H NMR.

One major advantage in the synthetic approach is using isoprene and DMB monomers instead of ethylene and propylene. While this requires hydrogenation to achieve the desired saturated copolymer, going through an unsaturated precursor is beneficial during characterization since the ethylene/propylene ratio can be determined easily by tracking the ratio of isoprene and DMB via ^{1}H NMR. This is possible due to the larger chemical shifts of the vinyl protons compared to the methylene. If ^{1}H NMR was taken on the saturated product, the peaks

corresponding to the methyl and methylene would have significant overlap due to the similar chemical environment, leading to poor resolution of individual peaks. This observation would be intensified due to the peak broadening, typically observed with polymers. Additionally, polyethylene- and polypropylene-based materials characteristically have poor solubility requiring the use of harsh organic solvents at high temperatures (xylenes or chlorinated benzenes at 140 °C) so solution-based characterization techniques would prove challenging and ineffective. The unsaturated intermediate copolymers were soluble in common solvents and allowed for more thorough characterization of the graft polymers prior to hydrogenation.

To determine the compatibility of the two monomers of interest, isoprene and DMB, a set of copolymerization reactions were performed with varying amounts of each monomer. ^{1}H NMR was used to track the monomer composition in the polymer chain. As the feed of isoprene increased, intensity corresponding to the vinyl proton found downfield near 5.1 ppm increased relative to the other peaks. By normalizing this integration value and comparing it to the protons found upfield at 2.0 ppm, a ratio of isoprene and DMB repeating units in the spectra could be determined using the equation shown (Figure 2.1).

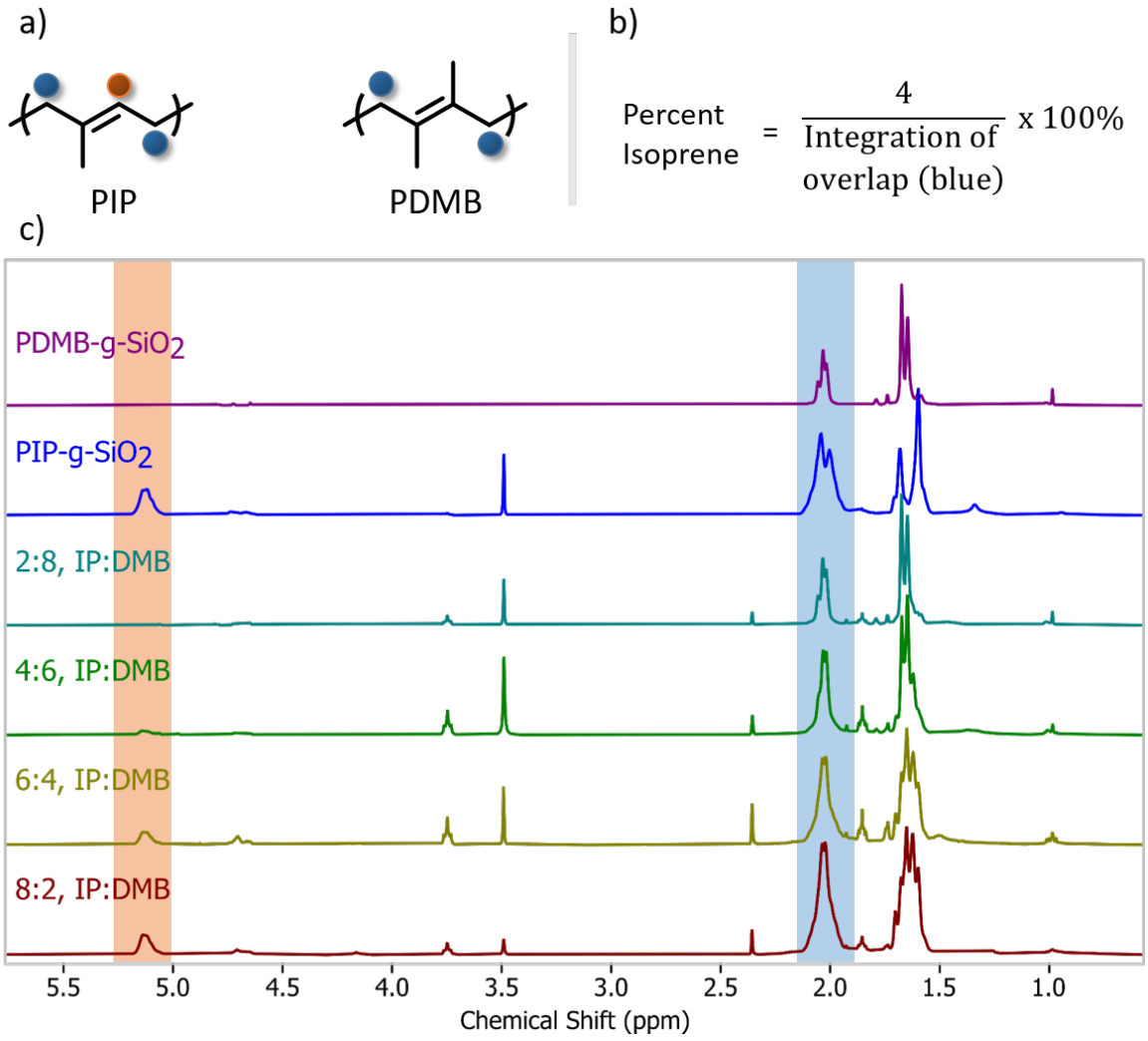

Figure 2.1: (a) Repeating units of polyisoprene (left) and PDMB (right), (b) Formula for percent isoprene calculation when integration value for vinyl proton is normalized to 1.0, (c) Stacked ^{1}H NMR spectra from the copolymerization of isoprene and DMB with vinyl proton (red) and allylic protons (blue) highlighted accordingly.

One challenge faced in development of this synthetic scheme pertains to the final step of hydrogenating the unsaturated polymer. This reaction was studied running the conditions with polyisoprene since the disappearance of the vinyl proton could easily be tracked. As seen in Figure 2.2, the vinyl proton found near

5.1 ppm is still present after the reaction, evident the reaction did not go to completion. Appearance of the new peaks found upfield near 0.9 ppm, however, is indicative the reaction did occur to some degree. Comparing the ratio of these two peaks, the degree of hydrogenation was determined to be approximately 73%. This was also performed with PDMB, and a similar result of partial hydrogenation was observed, with hydrogenation reaching only 25%. The higher percent hydrogenation of PIP over PDMB could be attributed to the increased sterics from the additional methyl group attached to the double bond.

Further investigation of the hydrogenation reaction was performed (Table 2.2); increasing the time from three hours to three days yielded only a slight increase in hydrogenation from 73 to 75%. Resubjecting a partially hydrogenated sample to identical conditions yielded no difference, and only resulted in unreacted *para*-toluenesulfonyl hydrazide (TSH) precipitating out during cooling of the reaction solution. This observation implied further addition of TSH would not prove effective. Also, increasing the amount of TSH could negatively impact the reaction as toluenesulfonyl anions have been known to attack siloxane bonds (Si – O – C) which would result in cleaving of polymer chains from the particle surface.[23] At the current conditions, cleaving of polymer brushes was more prominent on particles with lower graft density and molecular weight since looser brushes could not effectively shield the particle core. An alternative approach

toward improving hydrogenation used Wilkinson's Catalyst with hydrogen gas. This route proved ineffective as a hydrogenation level of only 26% was observed. While there were other variables that could be manipulated (i.e. pressure, time, heat, etc), it was decided use of Wilksinson's catalyst or any palladium catalyst did not pose a viable route as the high affinity of these metals and silica would result in challenging purification (Trial of hydrogenation reactions found in Table 2.2).

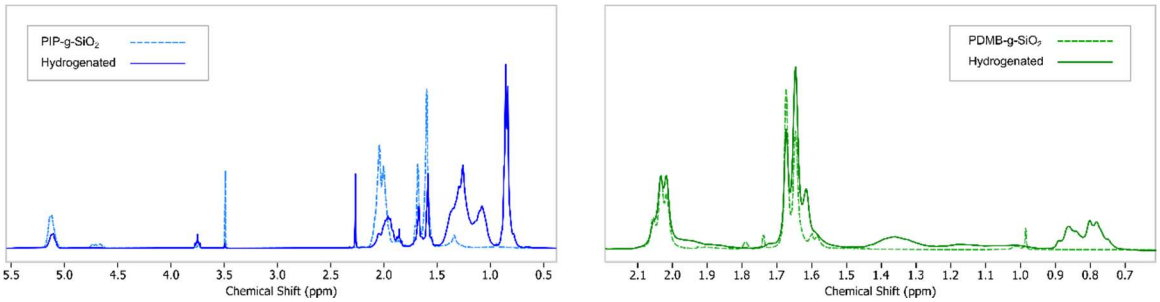

Figure 2.2: ^{1}H NMR spectra comparison of unsaturated polymer and after hydrogenation reaction of PIP (left) and PDMB (right).

Table 2.2: Hydrogenation trials and reaction conditions of PIP-g-SiO_2

Entry	Conditions	Degree of Hydrogenation	Notes
1	TSH	73%	145 °C, 3 hours
2	TSH	75%	145 °C, 3 hours, 2^{nd} reaction
3	TSH	75%	145 °C, 3 days
4	Wilkinson's	26%	8 h, 40 bar, 100 °C

A 1:1 copolymer of isoprene and DMB was synthesized by combining the successes of the previous studies (Figure 2.3). FTIR comparison of the unsaturated copolymer and hydrogenated product show that hydrogenation was successful

due to the significant decrease in the stretch intensities found at 3070 and 1644 cm^{-1} corresponding to the = C – H and C = C stretching, respectively. Additionally, ^{1}H NMR further supports this claim as the vinyl proton found at 5.1 ppm decreased dramatically after hydrogenation compared to the unsaturated counterpart. TGA comparison before and after hydrogenation were nearly identical in the ratio of polymer to nanoparticle weight%, indicating the grafted polymers were preserved in the reaction conditions. Finally, dynamic light scattering (DLS) was performed before and after polymerization. The narrow size distribution presented in both cases indicates aggregation was mitigated. Since only a low molecular weight

polymer (11.5 kDa) was grown onto the particle, significant changes in the particle size distribution was not expected.

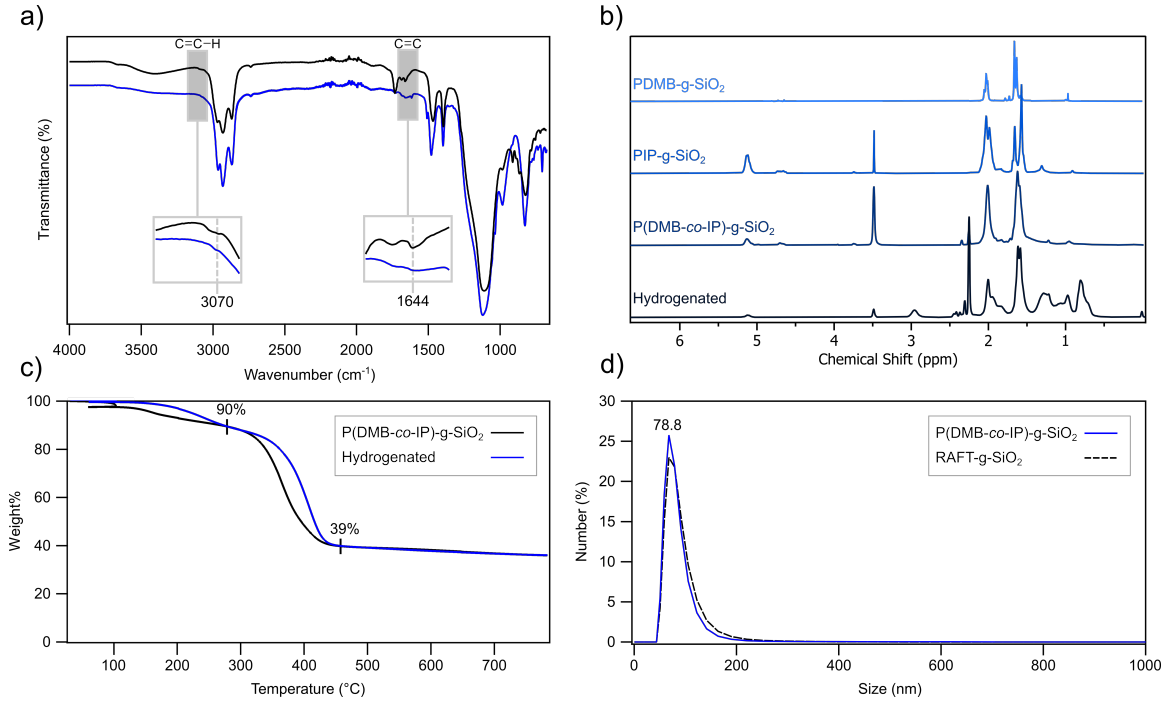

Figure 2.3: (a) FTIR of P(DMB-*co*-IP)-g-SiO_2 (black) and hydrogenated (blue); (b) stacked ^1H NMR of homopolymers, copolymer, and hydrogenated copolymer; (c) TGA before (black) and after (blue) hydrogenation; (d) DLS comparison of DoPAT-g-SiO_2 before (dashed black) and after (solid black) polymerization.

Table 2.3: Thermal Analysis of Polyolefin Nanocomposites

Entry	Graft Density (ch/nm²)	Isoprene Percentage[a]	Degree of Hydrogenation (%)[b]	T_g (°C)[c]	Thermal Stability (°C)[d]
1	0.060	13	32	-23.5/ -22.9	279
2	0.060	35	43	-34.6/ -25.8	272
3	0.060	56	53	-48.0/ -47.3	320
4	0.213	27	39	-19.4/ -24.0	296
5	0.213	39	45	-29.9/ -37.7	332

6	0.213	75	63	-44.1/ -53.9	347
7	0.318	28	39	-14.9/ -48.6	347
8	0.318	40	45	-30.6/ -32.4	305
9	0.318	71	61	-47.5/ -50.4	340

[a]Experimental isoprene percentage in DMB. [b]Estimated degree of hydrogenation based on maximum hydrogenation of homopolymers (25%, PDMB; 75%, PIP). [c]Glass transition temperature (DSC) of materials was expressed as before/after hydrogenation. [d]Determined via TGA by recording onset of curve from organic mass weight loss.

Further thermal analysis studies were performed on three set of nanoparticles with different graft densities and varying amounts of isoprene to DMB (Table 2.3). When running differential scanning calorimetry (DSC), only one glass transition temperature (T_g) feature was observed for each copolymer, suggestive of a random sequence (Figure 2.4 b, d, and f). As expected, T_g of the copolymers decreased as isoprene content increase due to the lower T_g of the homopolymers (*cis*-polyisoprene (-73 °C) and *cis*-polyDMB (2 °C)). These results also agree well with the calculated T_g's using the Fox Equation, e.g., Entry 3 and 8 calculated/experimental T_g's are -48/-49 °C and -31/-36 °C, respectively. After hydrogenation, only a slight change in T_g was observed, likely due to the modest degree of hydrogenation (~50%) for each copolymer. TGA shows loss of polymer mass is increased as polymer molecular weight decreases. This is seen when comparing the TGA curves of Figure 2.4 (a, c, and e); decreasing polymer molecular weight effectively reduces shielding of the nanoparticle core, thus

promoting polymer cleaving by the toluenesulfonyl anion. Estimation of hydrogenation was based on the %isoprene content and max hydrogenation of each homopolymer since the overlapping peaks on the ^{1}H NMR spectra made distinguishing between the four different species (saturated, unsaturated, isoprene, and DMB) unmanageable.

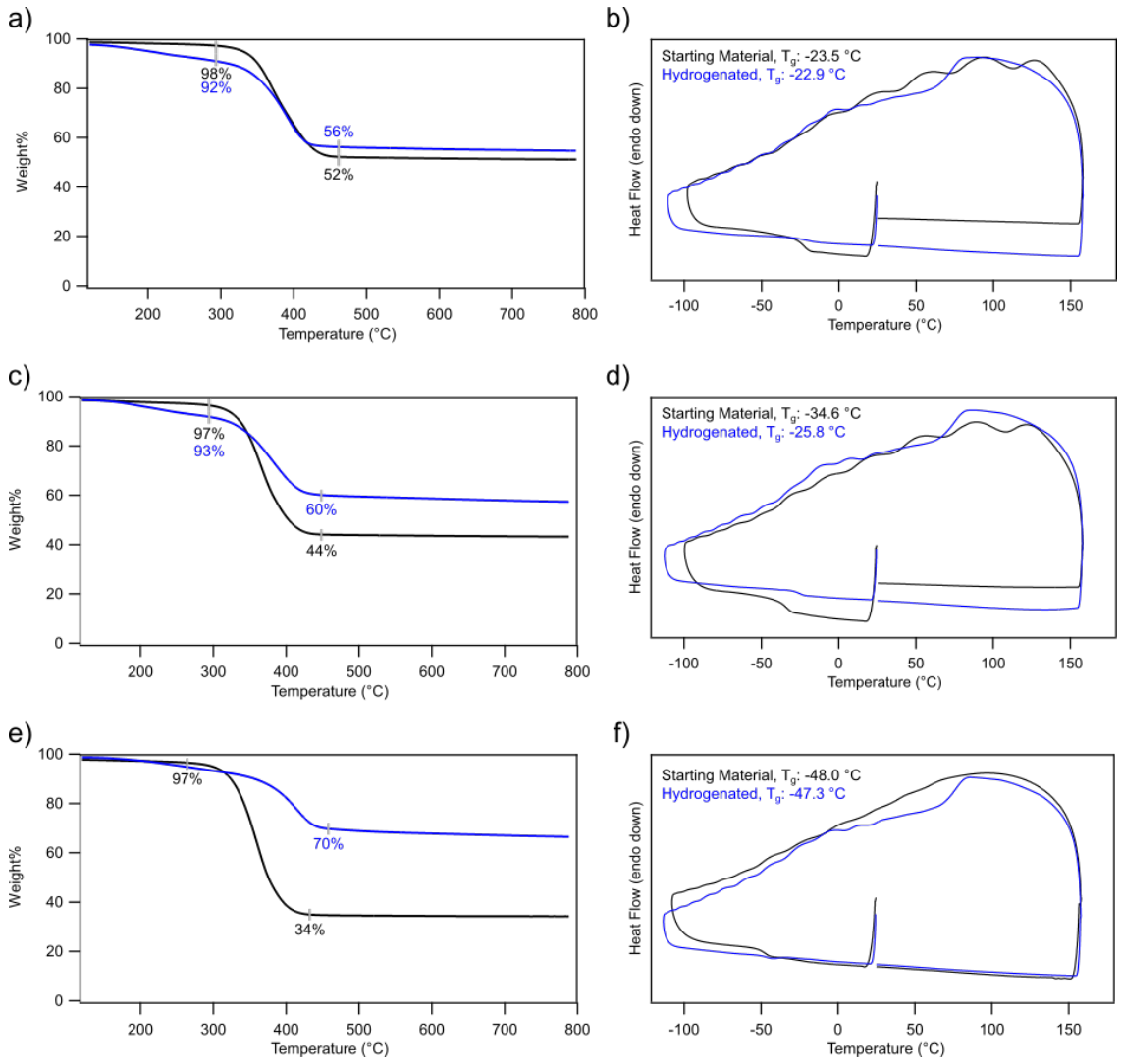

Figure 2.4: Thermal analysis of polymer nanocomposites with graft density: 0.060 ch/nm^2. TGA (left) and DSC (right) were performed before (black) and after hydrogenation (blue). Molecule weight decreases going from 98.1 kDa (Entry 1, a

and b), 65.9 kDa (Entry 2, c and d), and 47.9 kDa (Entry 3, e and f). Isoprene content increases going from 13% (Entry 1), 35% (Entry 2), and 56% (Entry 3).

2.5 Conclusions

In this work, a novel approach for an ethylene- and propylene-free synthesis of an ethylene/propylene copolymer grafted to silica nanoparticles was developed along with detailed characterization of the nanocomposite material. By utilizing SI-RAFT polymerization, controlled polymerization of isoprene and DMB could be achieved while demonstrating control over polymer molecular weight. Additionally, the resulting unsaturated copolymer of isoprene/DMB offers a material with high solubility and ease of polymer composition determination due to the greater differences in the chemical environments of the protons.

Hydrogenation of the isoprene-DMB precursors led to polymers with ethylene/propylene compositions with low T_g's and a controllable ratio of ethylene and propylene content. Development of this synthetic strategy toward olefin-based polymer nanocomposites is a powerful addition to the synthetic toolbox for polymer chemists as it utilizes well-established SI-CRP, and offers an alternative, more viable approach toward desirable ethylene/propylene copolymer nanocomposites.

2.6 References

1. *Chemical and Engineering News* **2018**, Vol. 96, Issue 25, pp 26-29.

2. Malpass, D. B.; Band, E. I. "Introduction to Polymers of Propylene," in *Introduction to Industrial Polypropylene: Properties, Catalysis, Processes.* (2012) Scrivener, pp. 1-18.

3. Geyer, R.; Jambeck, J. R.; Law, K. L. Production, Use, and Fate of All Plastics Ever Made. *Sci. Adv.* **2017**, No. 3, e1700782.

4. Bendjaouahdou, C.; Bensaad, S. Properties of Polypropylene/(Natural Rubber)/Organomontmorillonite Nanocomposites Prepared by Melt Blending. *Journal of Vinyl & Additive Technology* **2011**, *17*(1), 48-57.

5. Ismail, H.; Suryadiansyah. Properties of Polypropylene/Natural Rubber/Recycle Rubber Powder Blends. *Polymer-Plastics Technology and Engineering* **2007**, *5*, 833-845.

6. Li-L.-P.; Yin, B.; Yang, M.-B. Morphology Prediction and the Effect of Core-Shell Structure on the Rheological Behavior of PP/EPDM/HPDE Ternary Blends. *Polym. Eng. Sci.* **2011**, *51*, 2425-2433.

7. Zhou, Y.; Li, L.-P.; Yang, M.-B.; Feng, J.-M. Characterization of PP/EPDM/HDPE Ternary Blends: The Role of Two EPDM with Different Viscosity and Processing Method. *Polymer-Plastics Technology and Engineering* **2012**, *51*(10), 983-990.

8. Jiang, W.; Tjong, S. C.; Li, R. K. Y. *Polymer* **2000**, *44*, 3479.

9. Gao, X.; Mao, L.-X.; Jin, R.-G.; Zhang, L.-Q.; Tian, M. Structure and Mechanical Properties of PP/EPDM/Attapulgite Ternary Blends. *Polymer* **2007**, *39*(10), 1011-1017.

10. Akcora, P.; Liu, H.; Kumar, S. K.; Moll, J.; Li, Y.; Benicewicz, B. C.; Schadler, L. S.; Acehan, D.; Panagiotopoulos, A. Z.; Pryamitsyn, V.; Ganesan, V.; Ilavsky, J.; Thiyagarajan, P.; Colby, R. H.; Douglas, J. F. Anisotropic Self-Assembly of Spherical Polymer-Grafted Nanoparticles. *Nat. Mater.* **2009**, *8*, 354-359.

11. Natarajan, B.; Neely, T.; Rungta, A.; Benicewicz, B. C.; Schadler, L. S. Thermomechanical Properties of Bimodal Brush Modified Nanopartaicle Composites. *Macromolecules* **2013**, *46*, 4909-4918.

12. Walker, S. B.; Lewis, J. A. Reactive Silver Inks for Patterning High-Conductivity Features at Mild Temperatures. *J. Am. Chem. Soc.* **2012**, *134*, 1419-1421.

13. Xu, L. Y.; Yang, G. Y.; Jing, H. Y.; Wei, J.; Han, Y. D.; Ag-Graphene Hybrid Conductive Ink for Writing Electronics. *Nanotechnology* **2014**, *25*, 055201.

14. Liu, C. H.; Yu, X. Silver Nanowire-Based Transparent, Flexible, and Conductive Thin Films. *Nanoscale Res. Lett.* **2011**, *6*, 75.

15. Hore, M. J. A.; Korley, L. T. J.; Kumar, S. K. Polymer-Grafted Nanoparticles. *J. Appl. Phys.* **2020**, *128*, 030401.

16. Mackay, M. E.; Tuteja, A.; Duxbury, P. M.; Hawker, C. J.; Horn, B. V.; Guan, Z.; Chen, G.; Krishnan, R. S. General Strategies for Nanoparticle Dispersion. *Science* **2006**, *311*, 1740-1743.

17. He, F.-A.; Zhang, L.-M.; Jiang, H.-L.; Chen, L.-S. Wu, Q.; Wang, H.-H. A New Strategy to Prepare Polyethylene Nanocomposites Using a Late-Transition Metal Catalyst Supported on $AlEt_3$-Activated Organoclay. *Compos. Sci. Technol.* **2007**, *67*, 177-1733.

18. Ahn, S. H.; Kim, S. H.; Kim, B. C.; Shim, K. B.; Cho, B. G. Mechanical Properties of Silica Nanoparticles Reinforced poly(ethylene 2,6-naphthalate). *Macromolecular Research* **2004**, *12*(3), 293-302.

19. Xu, X.; Zou, Y.; He, J.; Zeng, Y.; Yu, C.; Zhang, F. Insight into the Effects of Reaction Conditions on Metal-Free Surface-Initiated Atom-Transfer Radical Polymerization of Methyl Methacrylate from SBA-15. *J. Appl. Phys.* **2020**, *127*, 11510.

20. Abbas, Z. M.; Khani, M. M.; Tawfilas, M.; Marsh, Z. M.; Stefik, M.; Benicewicz, B. C. Surface-Initiated RAFT Polymerization of 2,3-Dimethyl-1,3-butadiene on Silica Nanoparticles for Matrix-Free Rubber Nanocomposites. *J. of Polym. Sci.* **2020**, *58*, 417-427.

21. Khani, M. M.; Abbas, Z. M.; Benicewicz, B. C. Well-Defined Polyisoprene-Grafted Silica Nanoparticles via the RAFT Process. *J. of Polym. Sci, Part A: Polym. Chem.* **2017**, *55*, 1493-1501.

22. Hahn. S. F. An Improved Method for the Diimide Hydrogenation of Butadiene and Isoprene Containing Polymers. *J. of Polym. Sci.: Part A: Polym. Chem.* **1992**, *30*, 397-408.

23. Petzetakis, N.; Stone, G. M.; Balsara, N. P. Synthesis of Well-Defined Polyethylene-Polydimethylsiloxane-Polyethylene Triblock Copolymers by Diimide-Based Hydrogenation of Polybutadiene Blocks. *Macromolecules* **2014**, *14*(13), 4151-4159.

CHAPTER 3

POLYETHYLENE GRAFTED SILICA NANOPARTICLES VIA RAFT POLYMERIZATION[1]

[1]Ly, R. T.; and B. C. Benicewicz. To be submitted to *Macromolecules*.

3.1 Abstract

Progress in surface-initiated polymerizations has led to effective synthetic routes toward desirable polyolefin nanocomposites such as polyethylene grafted nanoparticles utilizing surface-initiated ring-opening metathesis polymerization (SI-ROMP). Through this approach, however, expanding polymer architecture is limited by the requirement of cyclic monomers with high ring strain, so preparing low ethylene content copolymers requires branched rings limiting the scope of potential polymers. RAFT polymerization is compatible with a significantly wider range of monomers, namely butadiene-based monomers. This work presents a novel ethylene-free synthesis of polyethylene-grafted nanoparticles via SI-RAFT with accurate graft density determination and controllable molecular weight of the grafted polymers. The synthesis and characterization of polyethylene nanocomposites along with challenges faced are discussed in detail.

3.2 Introduction

Polyethylene (PE) is the most produced commodity thermoplastic, and can be seen in everyday applications such as consumer goods and packaging.[1] PE is the typical choice of material for applications requiring chemical stability, high strength at low density, and moderate heat resistance. These desirable properties also come at low cost and ease of processing, making PE an extremely attractive candidate. The impressive strength of PE can be attributed to the semi-crystalline

nature of the polyolefin, and depending on the degree of branching, different grades of polyethylene can be achieved: high-density polyethylene (HDPE), lo-density polyethylene (LDPE), linear low-density polyethylene (LLDPE), etc.[2] Despite the impressive properties of PE, there exist few literature examples of polyethylene nanocomposites likely due to the challenges of grafting polyethylene onto particle surfaces. PE is commercially prepared through polymerization of ethylene gas using Ziegler-Natta catalysts. Using this coordination chemistry yields a polymer with broad molecular weight, but can also achieve excellent stereospecific control.[3-5] To effectively prepare polyethylene nanocomposites, controlling polymer brush architecture, i.e. polymer molecular weight and graft density, would be necessary to optimize properties of the material.[6-10] So, using well-controlled polymerization techniques to effectively grow polymer chains with predictable molecular weight and low dispersity would prove beneficial in the synthesis of polymer brushes.

In the development of controlled polymerization techniques, intricate architectures and functionality of polymer brushes have been explored;[11-13] however, despite these advances, controlled synthesis of polyethylene brushes has hardly been explored. Pribyl et al.[14] were able to effectively grow near perfectly linear polyethylene onto silica nanoparticles using surface-initiated ring-opening metathesis polymerization (SI-ROMP). By functionalizing the surface with

norbornene, Grubbs catalyst could be adhered to the surface, allowing for polymerization to occur from the surface. While effective in producing linear PE brushes, other functionalized polyethylenes proves challenging as ROMP is limited to cyclic monomers with ring strain.[15] To incorporate branching, substituted cyclic monomers would be required. This was demonstrated by Kobayashi et al.[16] In this work, cyclooctene monomers were prepared with various R groups substituted at the 3-position of the ring, and underwent ROMP to yield a set of LLDPEs. Due to the close proximity to the reactive double bond, increasing the size of the substituent negatively impacted degree of polymerization. So, using ROMP in synthesis of PE brushes has proven to be an effective approach; however, deviating away from linear PE poses a challenge due to the limitations in the choice of monomers.

Reversible addition-fragmentation chain transfer (RAFT) polymerization is a controlled radical polymerization reaction that works by introducing radical species to a chain transfer agent (CTA) known as a RAFT agent. In doing so, the RAFT agent undergoes an equilibrium between active and dormant states, and as long as this rate is higher than propagation, less than one monomer will be added onto the chain in each active state, resulting in each chain growing at the same rate. Through RAFT, predictable molecular weight and low dispersity are typically observed, and, unlike ROMP, a wide range of monomers is accessible.[17] With these

benefits in mind, using RAFT in synthesis of PE brushes would be ideal. Additionally, previous works have established efficient processes for surface-initiated RAFT (SI-RAFT) polymerization.[18-20] PE via RAFT polymerization was performed by Dommanget et al.[21] In this work, they were successful in polymerizing ethylene gas to form the desired PE; however, a maximum polymer molecular weight of only 2.0 kDa was achieved. This limitation was attributed to the poor solubility of the growing chain. Work by Frech et al.[21] demonstrated an ethylene-free approach toward PE. Here, they polymerized the monomer, *N*-(acryloyloxy)-phthalimide (AP), so once polymerized, the phthalimide moiety could be removed through photoinitiated decarboxylation. By going through the phthalimide precursor, higher molecular weight (relative to the previous approach) was achieved (~8.4 kDa) while avoiding use of toxic solvents (i.e. chlorinated benzenes). While higher molecular weight of the AP polymer was achieved (28 kDa), only partial decarboxylation was observed since decarboxylation led to precipitation from the solution. So, to effectively prepare PE nanocomposites, a precursor with high solubility should first be obtained to achieve high molecular weights. Afterwards, a post-polymerization reaction, with conditions still favorable for the insoluble product, could be performed to achieve the desired PE.

In this work, we present a new synthetic approach of an ethylene-free synthesis of polyethylene grafted to silica nanoparticles through SI-RAFT of 1,3-butadiene. Independently controlled graft density and molecular weight were achieved. The synthesis, characterization, and challenges during synthesis will be discussed.

3.3 Experimental

3.3.1 Materials and Instrumentation

Silica nanoparticles (MEK-ST, 30 wt.% in methyl ethyl ketone, diameter 14±4 nm) were donated by Nissan Chemical Corporation. Dry THF was obtained from a dry still solvent system and used immediately. All other chemicals were supplied by Thermo Fisher Scientific, Oakwood Chemicals, Alfa Aesar, Acros Organics, or Matrix Scientific. All chemicals were used as received unless stated otherwise. TGA was performed on a Hitachi Instrument STA7200 under nitrogen atmosphere in a platinum pan from 25 to 800 °C at a ramp of 10 °C/min. DSC was performed on a Hitachi Instrument DSC7020 under nitrogen atmosphere at a heating and cooling rate of 10 °C/min. Samples were sealed in aluminum pans for analysis. Two cycles were performed to erase previous thermal history of samples. ^{1}H NMR spectra were obtained from a Bruker Avance III-HD 300 MHz NMR in $CDCl_3$. UV-Vis spectroscopy was performed on a Shimadzu UV-2450 using an excitation wavelength of 360 nm. Scanning range was from 200 to 400 nm. Samples

were prepared in THF. FTIR was performed on a Perkin Elmer Spectrum 100 FT-IR Spectrometer equipped with a Universal ATR Sampling Accessory with runs set at 16 scans.

3.3.2 Activation of 2-(((dodecylthio)carbonothioyl)thio)propanoic Acid (DoPAT)

DoPAT (5.00 g, 14.3 mmol), 2-mercaptothiazoline (1.87 g, 15.7 mmol), and DCC (3.53 g, 17.1 mmol) were all combined in a 100 mL round-bottom flask and dissolved in dry THF (60 mL, 0.23 M). The solution was degassed by bubbling N_2 for 15 minutes. The solution was cooled to 0 °C using an ice bath. A solution of DMAP in THF (174 mg in 5 mL, 1.42 mmol) was added to the stirring solution via syringe. The solution was allowed to slowly reach room temperature and stirred for eight hours. The solution was then filtered to remove a salt by-product and the filtrate was collected, then concentrated under reduced pressure. The crude product was purified *via* column chromatography using a 30% ethyl acetate in hexanes solution as the mobile phase. Recrystallization was performed by dissolving the yellow oil in minimal amounts of THF followed by methanol and cooled to 0 °C overnight to yield a yellow precipitate. The yellow solid was collected and dried (4.19 g, 65%) ^{1}H NMR indicates a pure product. T_m = 33.8 °C (DSC). ^{1}H NMR (300 MHz, $CDCl_3$) δ 6.50-6.40 (q, 1H), 4.70-4.60 (m, 1H), 4.53-4.40

(m, 1H), 3.48-3.37 (m, 1H), 3.37-3.20 (m, 1H), 1.71-1.48 (m, 6H), 1.45-0.98 (m, 22H), 0.92-0.79 (t, 3H). ^{1}H NMR, ^{13}C NMR, and DSC curve found in Figure A.1-A.3.

3.3.3 Synthesis of DoPAT-*g*-SiO_2

A solution (20 g) of colloidal silica particles (30 wt% in methyl ethyl ketone) was added to a 100 mL round-bottom flask equipped with a stir bar and diluted with dry THF (20 mL). To the solution, (3-aminopropyl)dimethylethoxysilane, or aminosilane (375 μL, 1.99 μmol) and n-octyldimethylmethoxysilane, or octylsilane (160 μL, 0.643 μmol). The flask was capped with a rubber septum and secured with copper wire and the solution was degassed by bubbling argon for 15 minutes. The flask was then placed in an oil bath set at 70 °C and reacted for six hours. The solution was cooled to room temperature and the nanoparticles were precipitated from solution by the addition of hexanes followed by centrifugation of solution at 6,500 rpm for five minutes. The supernatant was discarded and the solids were re-dispersed in THF (20 mL). Activated DoPAT (180 mg, 0.40 mmol) was added and the solution was stirred for eight hours without presence of light. Afterwards, the nanoparticles were precipitated with the addition of methanol and centrifugation at 6,500 rpm for five minutes. The nanoparticles were re-dispersed in THF and this was repeated until the supernatant no longer had any color. The particles were dried overnight to yield large yellow solids. The particles were stored at -25 °C for

further use. UV-Vis was taken to determine graft density by observing the absorbance at 309 nm.

3.3.4 General Procedure for Free Polymerization of 1,3-butadiene with RAFT

To a 50 mL metal reactor, DoPAT (25 mg, 0.0713 mmol), a solution of dicumyl peroxide, or DCP in toluene (0.01 M, 1.07 mL), and 1,3-butadiene (ca. 15% in toluene) was added. The species of the reaction were held at a ratio of 2,500:1.0:0.15 with [monomer]:[CTA]:[initiator]. The metal reactor was placed in an oven equipped with a rotating apparatus and set at 150 °C for three days. The solution was allowed to cool to room temperature and the resulting polymer was collected by addition of methanol followed by centrifugation at 6,500 rpm for five minutes. The solids were re-dispersed in THF and this was repeated three times to remove impurities. The product was dried under reduced pressure.

3.3.5 General procedure for SI-RAFT Polymerization of 1,3-butadiene

In a typical polymerization, DoPAT-*g*-SiO_2 (100 mg) with a graft density of 53.9 μmol/g was dissolved in dry THF (5.0 mL). A solution of DCP in toluene (0.01 M, 800 μL) and 1,3-butadiene (ca. 15% in toluene) were added. The species of the reaction were held at a ratio of 2,500:1:0.15 with [monomer]:[CTA]:[initiator]. The solution was decanted into metal reactors and rotated in an oven set at 150 °C for three days. The solution was allowed to cool to room temperature and the resulting polymer grafted nanoparticles were collected by addition of methanol

followed by centrifugation at 6,500 rpm for five minutes. The solids were re-dispersed in THF and this was repeated three times to remove free polymer. The product was dried under reduced pressure and molecular weight was determined via TGA.

3.3.6 General Hydrogenation Reaction

In a typical reaction, the unsaturated polymer nanocomposite (1,500 mg, 22.46 mmol in respect to double bonds) and *o*-xylene (150 mL) were added to a round-bottom flask and dissolved at 90 °C. After a clear solution was observed, *para*-toluenesulfonyl hydrazide, or TSH (12.6 g, 67.38 mmol), and tri-n-propyl amine, or Pr_3N (12.4 mL, 67.38 mmol) were added. A condenser was attached and the solution was heated to 145 °C for three hours. The solution was then cooled to room temperature and the solution was decanted into methanol to yield a cloudy suspension. Centrifugation at 6,500 rpm for five minutes was performed to yield a yellow gel. Remaining solvents were removed under vacuum to yield a fine powder. ^1H was performed to determine degree of hydrogenation. TGA was performed to ensure grafted polymer was retained.

3.4 Results and Discussion

In this work, we present a synthetic strategy for ethylene-free synthesis of polyethylene grafted to silica nanoparticles with independent control over graft density and molecular weight (Scheme 3.1). To begin, silica nanoparticles were

functionalized with an aminosilane reagent at varying feed ratio along with an alkylsilane reagent to cap any unreacted silanol groups. The amine-functionalized nanoparticles were then reacted with an activated RAFT agent, DoPAT, to attach RAFT agents directly onto the surface. RAFT activation requires a DCC coupling reaction to promote reactivity of the carbonyl carbon over reaction with the trithioester. Varying the feed ratio of the aminosilane reagent allowed for tuning the graft density of particles prior to polymerization. Afterwards, polymerization was then performed from the nanoparticle surface using the monomer, 1,3-butadiene. To make this strategy feasible for typical organic laboratories, we focused on using commercially available reagents, particularly with the monomer; being a gas, use of butadiene adds requirement of specialized gaseous reaction vessels and increased amount of risk. For this work, a commercially available butadiene dissolved in toluene was used to mitigate these added consequences. Once polymerization occurs, the polymer-grafted nanoparticles were isolated and subjected to hydrogenation using TSH to convert the unsaturated polybutadiene (PBD) into the desired polyethylene grafted nanoparticles. A set of samples were prepared through this approach. Characterization data is shown in Table 3.1.

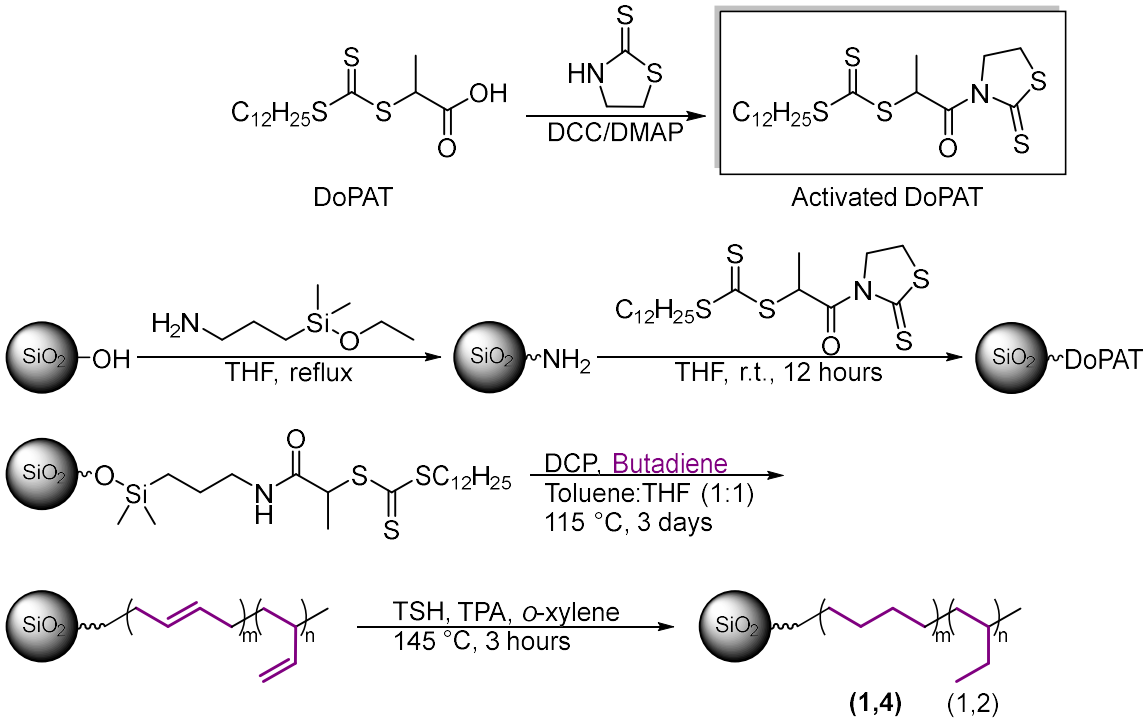

Scheme 3.1: Synthetic approach toward polyethylene grafted to silica nanoparticles

Table 3.1: Chemical and Physical Characteristics of PBD-*g*-SiO_2

Entry	Graft Density (ch/nm²)[a]	Reaction Time (hours)	Molecular Weight (kDa)[b]	Conversion (%)[c]	T_g (°C)[d]
1	0.060	3	16.3	12.1	-81.7
2	0.060	6	22.3	16.5	-80.0
3	0.060	8	18.2	13.5	-79.5
4	0.213	3	10.6	7.8	-78.0
5	0.213	6	17.6	13.0	-77.0
6	0.213	8	19.0	14.1	-77.0

Polymerizations were all performed at a ratio [Monomer]:[CTA]:[Initiator] of 2,500:1.0:0.15. [a]Graft density was determined prior to polymerization *via* UV-Vis. [b]Molecular weight was determined via TGA by comparing polymer mass ratio

with graft density. [c]Conversion percentage based on molecular weight of 100% converted monomer: 133.2 kDa. [d]Glass Transition Temperature (DSC).

One important benefit of this approach is the ability to determine graft density prior to polymerization. Unlike other surface-initiated polymerization techniques, e.g. SI-ATRP and SI-ROMP, concentration of RAFT agents functionalized to the nanoparticle surface can be quantified via UV-Vis; by comparing the absorbance of RAFT-*g*-SiO_2 to a calibration curve made using known quantities of the free RAFT agent, the concentration of RAFT agents for a known mass of nanoparticles can be determined and used to calculate the graft density (Figure 3.1).

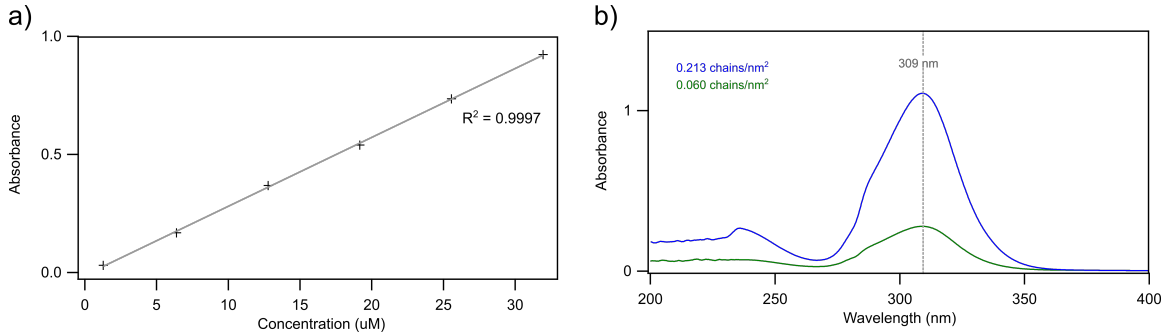

Figure 3.1: (a) Calibration curve of the RAFT agent, DoPAT and (b) UV-Vis spectra of nanoparticles used in polymerizations.

Determining graft density prior to polymerization offers an alternative method to determine polymer molecular weight using TGA. This is done by comparing the ratio of polymer to silica mass:

$$\text{Polymer MW} = \frac{\text{TGA}_{\text{polymer}}}{\left(\frac{\text{Graft Density} \times \text{SA}_{total}}{\text{N}_\text{A}}\right) \times \text{TGA}_{\text{nanoparticle}}}$$

where,

$$SA_{total} = \frac{SA_{sphere}}{V_{sphere} \times \rho_{SiO_2}}$$

where, $TGA_{polymer}$ is the percent mass of polymer, N_A is Avogadro's number, $TGA_{nanoparticle}$ is the percent mass of nanoparticle, and density (ρ) of SiO_2 is 2.3 g/cm^3. Using this approach, a kinetic study was performed using two different [monomer]:[CTA] ratios (Figure 3.2a). As expected, increasing the ratio from 1,000 to 2,500 offered faster rate of chain growth. Additionally, a higher molecular weight was also achieved. As mentioned previously, this work utilizes commercially available 1,3-butadiene, and as a result, a traditional kinetic study using ^{1}H NMR to monitor monomer consumption could not be performed with this system due to the highly volatile nature of the monomer; when attempted, the measured "monomer consumption" was inflated drastically depicting near 100% conversion only after several hours. Because of this, samples for the kinetic study were obtained using discrete reactions prepared from a mother solution and quenched at the specified times. ^{1}H NMR of neat PBD shows several peaks near 4.5 – 5.0 ppm corresponding to 1,2- and 1,4-addition, where 79% are 1,4- and 21% are 1,2-addition (Figure 3.2b). The higher percent of 1,2-addition could be attributed to oxygen in the system; removing air in the system with air-free manipulation techniques, e.g., freeze-pump-thaw, bubbling, cannot be used as the monomer would be removed along with the undesired oxygen.

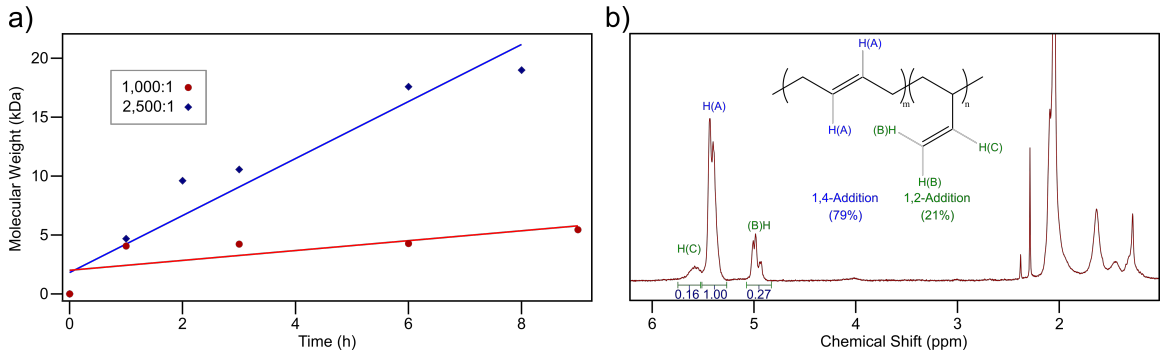

Figure 3.2: (a) Kinetic study of 1,3-butadiene polymerization onto silica nanoparticles. Polymerizations were conducted using two different ratios where [monomer]:[CTA]:[Initiator] = 1,000:1.0:0.15 (red circles) and 2,500:1.0:0.15 (blue diamonds). (b) ^{1}H NMR of neat PBD showing 1,4- and 1,2-addition.

Table 3.2: Thermal analysis of hydrogenated PBD-*g*-SiO_2

Entry	Graft Density (ch/nm^2)	Molecular Weight (kDa)	Char Yield (%)[a]	T_c (°C)[b]	T_m (°C)[c]
1	0.060	16.3	76/69	-	-
2	0.060	22.3	70/68	-	-
3	0.060	18.2	74/90	-	-
4	0.213	10.6	46/53	49.5	66.4
5	0.213	17.6	46/48	53.0	73.7
6	0.213	19.0	44/53	44.9	64.2

[a]Char yield expressed as "before/after" referring to before and after hydrogenation. [b]Crystallization point (DSC). [c]Melting point (DSC).

Hydrogenation conditions were performed on a set of PBD-*g*-SiO_2 samples, and thermal analysis was conducted on the unsaturated PBD-*g*-SiO_2 and reduced products (Table 3.2). The physical appearance changes significantly after hydrogenation from a sticky, gel-like material to a fine powder, comparable to

high-density polyethylene. TGA displays grafted polymers were preserved during hydrogenation conditions as curves corresponding to before and after align fairly well (Figure 3.3). DSC curves for the PBD nanocomposites show a clear T_g feature near -78 °C. Perfectly linear PBD (1,4-addition) has a T_g near -107 °C where 1,2-addition shows up at a higher temperature (0 °C). The theoretical T_g (-90 °C) calculated using Fox Equation of the 1,4-/1,2- "copolymer" agrees well using the mass ratio from ^{1}H NMR. Unlike substituted butadiene monomers (i.e. isoprene and 2,3-dimethyl-1,3-butadiene), hydrogenation of PBD yields near complete hydrogenation.[22]

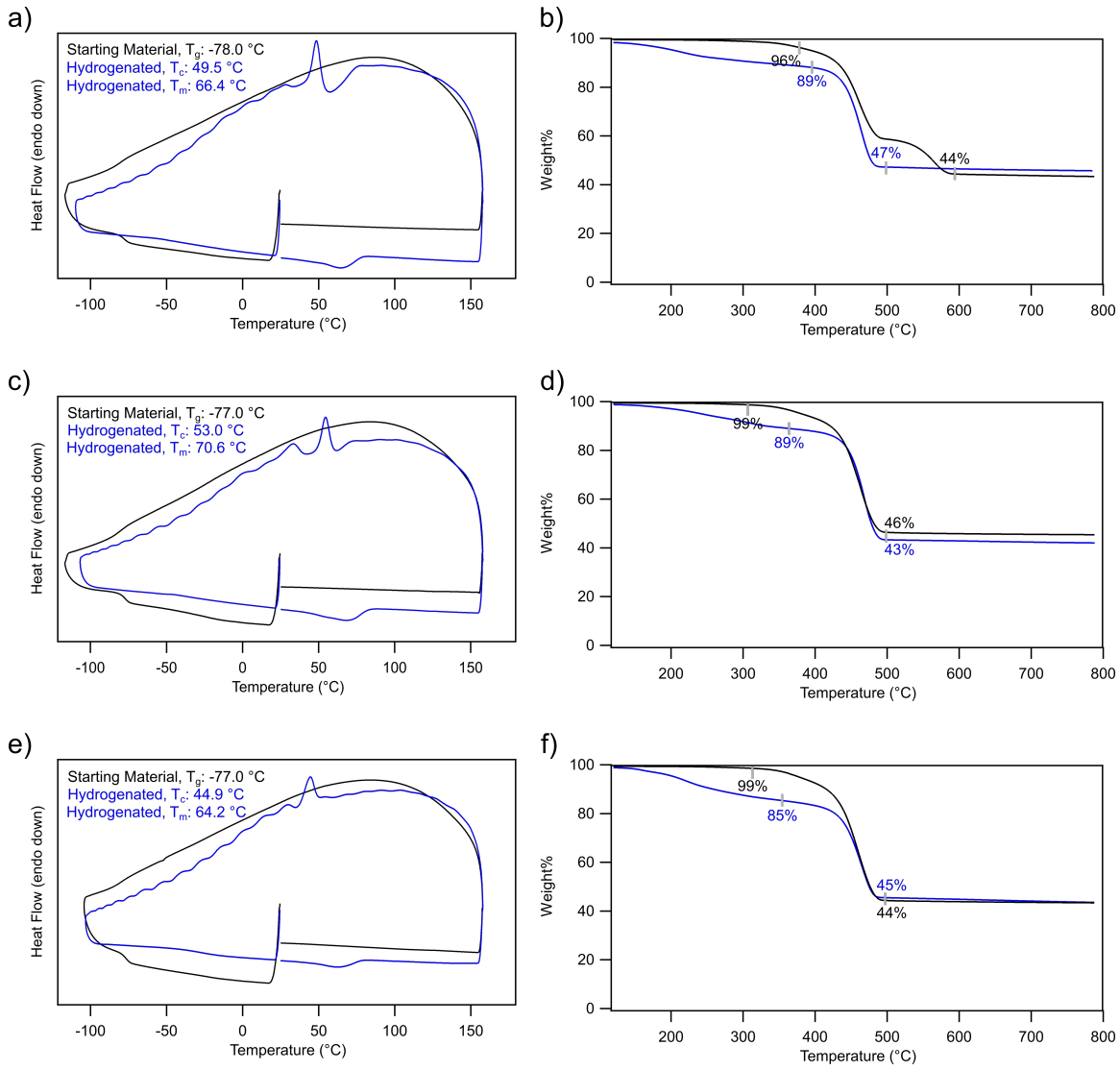

Figure 3.3: Thermal analysis of polymer nanocomposites with graft density: 0.213 ch/nm^2. DSC (left) and TGA (right) were performed before (black) and after hydrogenation (blue). MW of the samples are (a) 10.6 kDa, (c) 17.6 kDa, and (e) 19.0 kDa.

Post-hydrogenation, DSC curves show disappearance of T_g feature near -78 °C along with an appearance of a crystallization peak and melting peak near 52 °C and 71 °C, respectively (Figure 3.4b and c). In comparison, the melting point of low-density polyethylene (110 °C) and high-density polyethylene (132 °C) are

notably higher than the materials presented here. This observation is likely credited to the high degree of branching, a result of the 1,2-addition. Additionally, it should be noted the lack of peaks on the DSC curve for the materials prepared with graft density of 0.060 ch/nm^2 (Figure 3.4a). Compared to higher graft density samples (0.213 ch/nm^2) and neat polymer, it's expected DSC would not show features corresponding to the polymer since the relative polymer mass is significantly lower on low graft density particles.

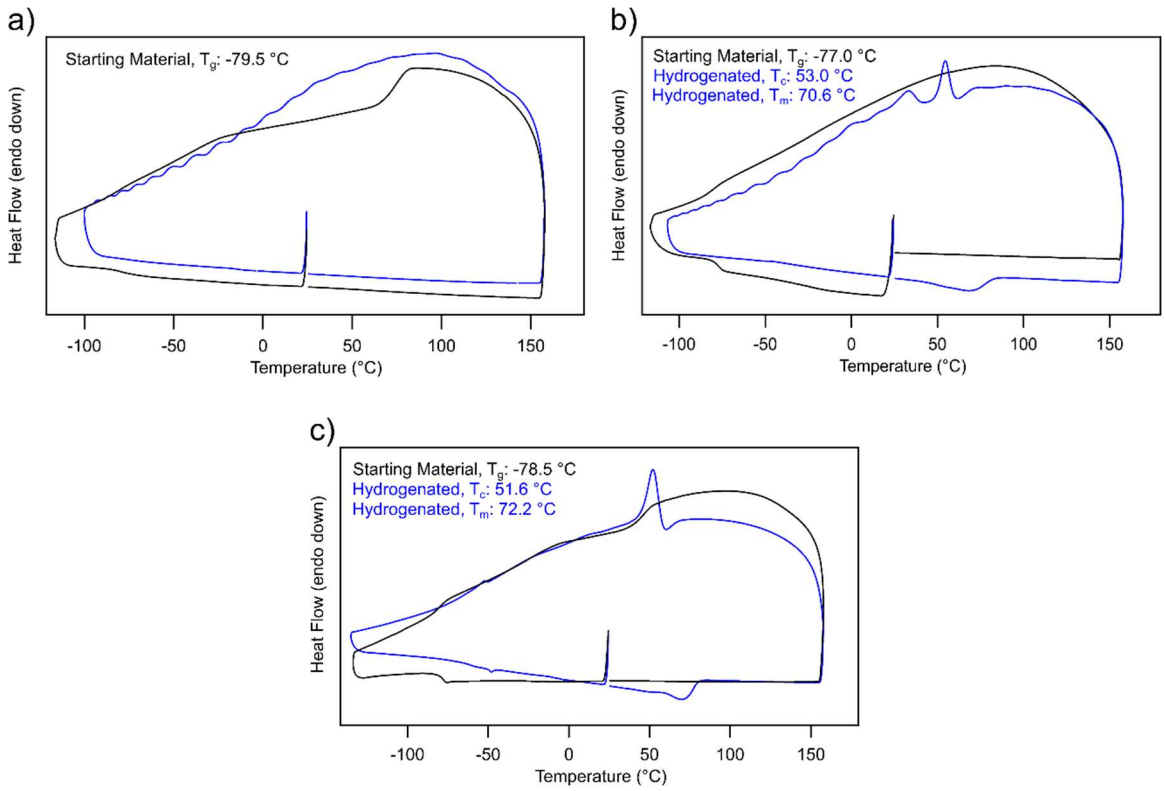

Figure 3.4: DSC curves of PBD on (a) 0.060 ch/nm^2 SiO_2 NP, (b) 0.213 ch/nm^2 SiO_2 NP, and (c) neat polymer. MW of three samples were similar: (a) 18.2 kDa, (b) 19.0 kDa, (c) 20.2 kDa.

3.5 Conclusions

In this work, a novel approach for an ethylene-free synthesis of polyethylene-grafted silica nanoparticles was developed along with detailed characterization of the process. By utilizing SI-RAFT polymerization, graft density could be determined prior to polymerization, thus offering an alternative method for polymer molecular weight calculations. The unsaturated precursor, PBD-*g*-SiO_2, was synthesized with controllable molecular weight and modest branching from the 1,2-addition.

Hydrogenation of the branched PBD-*g*-SiO_2 led to PE-*g*-SiO_2 with low melting point relative to commercially available PE products. Crystallinity was still achieved despite the defects present. Hydrogenation of the double bonds proceeded to a higher degree than was previously observed for isoprene and 2,3-dimethyl-1,3-butadiene polymers due to the lower steric hindrance and appeared to be nearly quantitative as determined by NMR. Development of this synthetic strategy toward grafted polyethylene nanocomposites is a great contribution to the synthetic toolbox of SI-CRP, offering an effective alternative to incorporate ethylene into nanocomposites without involving niche and high pressure gas reactors.

3.6 References

1. Geyer, R.; Jambeck, J. R.; Law, K. L. Production, Use, and Fate of All Plastics Ever Made. *Science Advances*. **2017**, *3*(7), 1-5.

2. Nowlin, T. E.; Mink, R. I.; Kissin, Y. V. Supported Magnesium/Titanium-Based Ziegler Catalysts for Production of Polyethylene. In *Handbook of Transition Metal Polymerization Catalysts*, online ed.; Hoff, R., Mather, R. T.; John Wiley & Sons: Hoboken, NJ, 2010; p 131.

3. Eisch, J. J. Fifty Years of Ziegler-Natta Polymerization: From Serendipity to Science. A Personal Account. *Organometallics*, **2012**, *31*, 4917-4932.

4. Busico, V.; Cipullo, R.; Friederichs, N.; Ronca, S.; Talarico, G.; Togrou, M.; Wang, B. Block Copolymers of Highly Isotactic Polypropylene via Controlled Ziegler-Natta Polymerization. *Macromolecules*, **2004**, *37*, 8201-8203.

5. Zhang, J.; Nan, F.; Yu, H.; Zhang, S.; Xia, X.; Huang, Q.; Yi, J.; Li, H.; Zhao, Z. Direct Preparation of Transparent Isotactic Polypropylene with Supported Ziegler-Natta Catalysts Containing Novel Eco-friendly Internal Electron Donors. *Ind. Eng. Chem. Res.* **2020**, *59*(19), 8995-9003.

6. Hore, M. J. A.; Korley, L. T. J.; Kumar, S. K. Polymer-Grafted Nanoparticles. *J. Appl. Phys.* **2020**, *128*, 030401.

7. Bansal, A.; Yang, H.; Li, C.; Benicewicz, B.; Kumar, S. K.; Schadler, L. S. Controlling the Thermomechanical Properties of Polymer Nanocomposites by Tailoring the Polymer-Particle Interface. *J. of Polym. Sci: Part B: Polym Phys*, **2006**, *44*, 2944-2950.

8. Mackay, M. E.; Tuteja, A.; Duxbury, P. M.; Hawker, C. J.; Horn, B. V.; Guan, Z.; Chen, G.; Krishnan, R. S. General Strategies for Nanoparticle Dispersion. *Science* **2006**, *311*, 1740-1743.

9. Zhao, B.; Brittain, W. J. Polymer Brushes: Surface-Immobilized Macromolecules. *Prog. Polym. Sci.* **2000**, *25*(5), 677-710.

10. Feng, C.; Huang, X. Polymer Brushes: Efficient Synthesis and Applications. *Acc. Chem. Res.* **2018**, *51*, 2314-2323.

11. Ballauff, M.; Borisov, O. Polyelectrolyte Brushes. *Curr. Opin. Colloid Interface Sci.* **2006**, *11*(6), 316-323.

12. Krishnan, S.; Weinman, C. J.; Ober, C. K. Advances in Polymers for Anti-Biofouling Surfaces. *J. Mater. Chem.* **2008**, *18*(29), 3405.

13. Civantos, A.; Martinez-Campos, E.; Nash, M. E.; Gallardo, A.;Ramos, V.; Aranaz, I. Polymeric and Non-Polymeric Platforms for Cell Sheet Detachment. *Adv. Mater. Interfaces* **2016**, 463-495.

14. Pribyl, J.; Benicewicz, B.; Bell, M.; Wagener, K.; Ning, X.; Schadler, L.; Jimenez, A.; Kumar, S. Polyethylene Grafted Silica Nanoparticles Prepared via Surface-Initiated ROMP. *ACS Macro Lett.* **2019**, *8*, 228-232.

15. Walker, R.; Conrad, R. M.; Grubbs, R. H. The Living ROMP of trans-Cyclooctene. *Macromolecules* **2009**, *42*, 599-605.

16. Kobayashi, S.; Pitet, L. M.; Hillmyer, M. A. Regio- and Stereoselective Ring-Opening Metathesis Polymerization of 3-Substituted Cyclooctenes. *J. Am. Chem. Soc.* **2011**, *133*, 5794-5797.

17. Perrier, S. 50th Anniversary Perspective: RAFT Polymerization – A User Guide. *Macromolecules* **2017**, *50*, 7433-7447.

18. Moad, G. Trithiocarbonates in RAFT Polymerization, RAFT Polymerization, 10.1002/9783527821358, (359-492), (2021).

19. Abbas, Z. M.; Khani, M. M.; Tawfilas, M.; Marsh, Z. M.; Stefik, M.; Benicewicz, B. C. Surface-Initiated RAFT Polymerization of 2,3-Dimethyl-1,3-butadiene on Silica Nanoparticles for Matrix-Free Rubber Nanocomposites. *J. of Polym. Sci.* **2020**, *58*, 417-427.

20. Khani, M. M.; Abbas, Z. M.; Benicewicz, B. C. Well-Defined Polyisoprene-Grafted Silica Nanoparticles via the RAFT Process. *J. of Polym. Sci, Part A: Polym. Chem.* **2017**, *55*, 1493-1501.

21. Frech, S.; Molle, E.; Butzelaar, A. J.; Theato, P. Ethylene-Free Synthesis of Polyethylene Copolymers and Block Copolymers. *Macromolecules* **2021**, *54*, 9937-9946.

22. Hahn. S. F. An Improved Method for the Diimide Hydrogenation of Butadiene and Isoprene Containing Polymers. *J. of Polym. Sci.: Part A: Polym. Chem.* **1992**, *30*, 397-408.

CHAPTER 4

ETHYLENE/PROPYLENE COPOLYMER NANOCOMPOSITES WITH HIGH ETHYLENE CONTENT THROUGH RAFT COPOLYMERIZATION OF 1,3-BUTADIENE AND ISOPRENE[1]

[1]Ly, R. T.; and B. C. Benicewicz. To be submitted to *Macromolecules*.

4.1 Abstract

Recent advances in surface-initiated polymerization chemistry has given rise to a library of polymer nanocomposite materials with complex brush architecture. Less complex polymers, namely polyolefin materials account for the majority of commodity thermoplastics produced worldwide. Despite the widespread use of these polyolefin materials and current techniques for surface-initiated controlled polymerization, few examples exist combining these two aspects. Synthesis of ethylene/propylene copolymers grafted to a surface poses a challenge in the field of nanocomposites. Presented here is a synthetic approach for ethylene/propylene copolymers with high ethylene content grafted to silica nanoparticles. Obtaining an unsaturated precursor offers facile route toward determination of polymer composition through solution-based characterization techniques. Controllable ethylene/propylene ratio was demonstrated through use of isoprene and BD monomers followed by mild hydrogenation conditions. Synthesis, characterization, and challenges faced are discussed.

4.2 Introduction

Polyethylene and polypropylene are the leading commodity thermoplastics produced worldwide, producing more than 70 million and 50 million metric tons each year, respectively. The high volume of these plastics can be attributed to low cost, ease of processing, paired with impressive mechanical strength and chemical

stability.[1-2] However, the widespread use of plastics has led to an alarming amount ending up as solid waste accumulating in the environment. Various approaches have been developed,[3-6] with one notable approach to improve miscibility amongst polymer blends, vastly improving reduction of waste with lower sorting costs. The incompatible nature of many polymer blends results in poor mechanical properties, inferior chemical and thermal stability, along with aging behavior compared to the original constituents.[7-9] These non-ideal properties are a consequence of phase separation between the polymers. As a result, polyolefin compatibilization has been explored for the past three decades to improve miscibility.[10-14] An effective strategy is addition of a copolymer to a blend with structural similarities of each individual polymer component, and to effectively combat the problem of polymer waste, the obvious pair to tackle would be polyethylene/polypropylene using ethylene/propylene copolymers.

Well-defined Ethylene/propylene block copolymers were prepared by metallocene coordination polymerization using a pyridylamidohafnium catalyst, and were added to a 30%/70% blend of HDPE and *i*PP to enhance impact strength almost matching that of neat HDPE.[15, 16] Similarly, a PE-*i*PP graft copolymer was prepared through copolymerization of ethylene gas and a polypropylene macromonomer. In doing so, improved tensile strength of the blend was observed with the addition of the copolymer.[17] A similar PE-*g*-PP graft copolymer was

prepared through ROMP of an atactic polypropylene macromonomer with cyclooctene. Unlike the previous methods, this approach gave a nearly random distribution, resulting in a more amorphous material.[18] Additional examples of ethylene/propylene copolymers also exist.[19-21]

Incorporation of nanofillers in polymer waste has proven to be a powerful strategy, with several examples of reinforcing polypropylene waste resulting in improved mechanical properties.[22-25] Silica nanoparticles are an attractive material in the field of nanocomposite chemistry since it's commercially available and easily synthesized. To optimize the properties of polymer nanocomposites, control over graft density and molecular weight must be achieved to effectively manipulate dispersion in a polyolefin matrix.[26-28]

Synthesis of ethylene/propylene copolymers raises two challenges: 1) accurate polymer composition determination, and 2) controllable copolymerization with predictable ratio. In previous examples,[15, 17] block copolymer architecture was commonly utilized as characterization could be performed at the end of each polymerization reaction. This route is limiting as the characterization of semi-crystalline polymers require use of high-temperature characterization techniques. Early work explored use of random ethylene/propylene copolymers through uncontrolled polymerization techniques.[10] However, due to the complexity of the copolymer from the

uncontrolled chain shuttling chemistry and high degree of variability for chain length and composition, establishing a fundamental understanding of the system posed a challenge. In this work, we present a new synthetic approach for ethylene/propylene copolymers grafted to silica nanoparticles utilizing SI-RAFT. By obtaining an unsaturated precursor, solution-based characterization techniques can be used to accurately determine polymer composition. Additionally, use of RAFT polymerization offers a platform for controlled synthesis of the copolymers, and independent variability of molecular weight and graft density. The synthesis, characterization, and challenges during synthesis will be discussed.

4.3 Experimental

4.3.1 Materials and Instrumentation

Silica nanoparticles (MEK-ST, 30 wt.% in methyl ethyl ketone, diameter (14±4 nm) were donated by Nissan Chemical Corporation. Dry THF was obtained from a dry still solvent system and used immediately. All other chemicals were supplied by Thermo Fisher Scientific, Oakwood Chemicals, Alfa Aesar, Acros Organics, Gelest, or Matrix Scientific. All chemicals were used as received unless stated otherwise. Isoprene was prepared by filtering through a basic alumina column to remove the inhibitor. TGA was performed on a Hitachi Instrument STA7200 under nitrogen atmosphere in a platinum pan from 25 to 800 °C at a ramp

of 10 °C/min. DSC was performed on a Hitachi Instrument DSC7020 under nitrogen atmosphere at a heating and cooling rate of 10 °C/min. Samples were sealed in aluminum pans for analysis. Two cycles were performed to erase previous thermal history of samples. ^{1}H NMR spectra were obtained from a Bruker Avance III-HD 300 MHz NMR in $CDCl_3$. UV-Vis spectroscopy was performed on a Shimadzu UV-2450 using an excitation wavelength of 360 nm. Scanning range was from 200 to 400 nm. Samples were prepared in THF. Dynamic light scattering (DLS) measurements were run on a Malvern Zetasizer instrument in glass cuvettes at a scattering angle of 90° with THF as the solvent. Fourier-Transform Infrared Spectroscopy (FTIR) was performed on a Perkin Elmer Spectrum 100 FT-IR Spectrometer equipped with a Universal ATR Sampling Accessory with runs set at 16 scans.

4.3.2 Activation of 2-(((dodecylthio)carbonothioyl)thio)propanoic Acid (DoPAT)

DoPAT (5.00 g, 14.3 mmol), 2-mercaptothiazoline (1.87 g, 15.7 mmol), and N,N′-dicyclohexylcarbodiimide (DCC) (3.53 g, 17.1 mmol) were all combined in a 100 mL round-bottom flask and dissolved in dry THF (60 mL, 0.23 M). The solution was degassed by bubbling N_2 for 15 minutes. The solution was cooled to 0 °C using an ice bath. A solution of 4-dimethylaminopyridine (DMAP) in THF (174 mg in 5 mL, 1.42 mmol) was added to the stirring solution via syringe. The solution was

allowed to slowly reach room temperature and stirred for eight hours. The solution was then filtered to remove a salt by-product and the filtrate was collected, then concentrated under reduced pressure. The crude product was purified *via* column chromatography using a 30% ethyl acetate in hexanes solution as the mobile phase. Recrystallization was performed by dissolving the yellow oil in minimal amounts of THF followed by methanol and cooled to 0 °C overnight to yield a yellow precipitate. The yellow solid was collected and dried (4.19 g, 65%) ^{1}H NMR indicates a pure product. T_m = 33.8 °C (DSC). ^{1}H NMR (300 MHz, $CDCl_3$) δ 6.50-6.40 (q, 1H), 4.70-4.60 (m, 1H), 4.53-4.40 (m, 1H), 3.48-3.37 (m, 1H), 3.37-3.20 (m, 1H), 1.71-1.48 (m, 6H), 1.45-0.98 (m, 22H), 0.92-0.79 (t, 3H). ^{1}H NMR, ^{13}C NMR, and DSC curve found in Figure A.1-A.3.

4.3.3 Synthesis of DoPAT-*g*-SiO_2

A solution (20 g) of colloidal silica particles (30 wt% in methyl ethyl ketone) was added to a 100 mL round-bottom flask equipped with a stir bar and diluted with dry THF (20 mL). To the solution, (3-aminopropyl)dimethylethoxysilane, or aminosilane (375 μL, 1.99 μmol) and n-octyldimethylmethoxysilane, or octylsilane (160 μL, 0.643 μmol). The flask was capped with a rubber septum and secured with copper wire and the solution was degassed by bubbling argon for 15 minutes. The flask was then placed in an oil bath set at 70 °C and reacted for six hours. The solution was cooled to room temperature and the nanoparticles were precipitated

from solution by the addition of hexanes followed by centrifugation of solution at 6,500 rpm for five minutes. The supernatant was discarded and the solids were re-dispersed in THF (20 mL). Activated DoPAT (180 mg, 0.40 mmol) was added and the solution was stirred for eight hours without presence of light. Afterwards, the nanoparticles were precipitated with the addition of methanol and centrifugation at 6,500 rpm for five minutes. The nanoparticles were re-dispersed in THF and this was repeated until the supernatant no longer had any color. The particles were dried overnight to yield large yellow solids. The particles were stored at -25 °C for further use. UV-Vis was taken to determine graft density by observing the absorbance at 309 nm.

4.3.4 General Procedure for Free Polymerization of 1,3-butadiene (BD) and Isoprene with RAFT

To a 50 mL metal reactor, DoPAT (25 mg, 0.0713 mmol), a solution of DCP in toluene (0.01 M, 1.07 mL), and a combination of isoprene and BD were added. The species of the reaction were held at a ratio of 2,500:1.0:0.15 with [monomer]:[CTA]:[initiator] where [monomer] is the combined ratio between the isoprene and BD. The metal reactor was placed in an oven equipped with a rotating apparatus and set at 150 °C for three days. The solution was allowed to cool to room temperature and the resulting polymer was collected by addition of methanol followed by centrifugation at 6,500 rpm for five minutes. The solids were

re-dispersed in THF and this was repeated three times to remove impurities. The product was dried under reduced pressure and the polymer composition was determined using ^{1}H NMR.

4.3.5 General procedure for SI-RAFT Copolymerization of BD and Isoprene

In a typical polymerization, DoPAT-*g*-SiO_2 (100 mg) with a graft density of 53.9 μmol/g was dissolved in dry THF (5.0 mL). A solution of DCP (0.01 M, 800 μL) with a combination of isoprene and DMB depending on the desired ethylene:propylene ratio was added. The species of the reaction were held at a ratio of 2,500:1:0.15 with [monomer]:[CTA]:[initiator] where [monomer] is the combined ratio between the isoprene and BD. The solution was decanted into metal reactors and rotated in an oven set at 115 °C for four days. The solution was allowed to cool to room temperature and the resulting polymer grafted nanoparticles were collected by addition of methanol followed by centrifugation at 6,500 rpm for five minutes. The solids were re-dispersed in THF and this was repeated three times to remove free polymer. The product was dried under reduced pressure and molecular weight was determined via TGA and polymer composition was determined using ^{1}H NMR.

4.3.6 General Hydrogenation Reaction

In a typical reaction, the unsaturated copolymer nanocomposite (1,500 mg, 22.46 mmol in respect to double bonds) and *o*-xylene (150 mL) were added to a

round-bottom flask and dissolved at 90 °C. After a clear solution was observed, TSH (12.6 g, 67.38 mmol), and tri-*n*-propyl amine, or Pr_3N (12.4 mL, 67.38 mmol) were added. A condenser was attached, and the solution was heated to 145 °C for three hours. The solution was then cooled to room temperature and the solution was decanted into methanol to yield a cloudy suspension. Centrifugation at 6,500 rpm for five minutes was performed to yield a yellow gel. Remaining solvents were removed under vacuum to yield a transparent gel. ^1H NMR was performed to determine degree of hydrogenation.

4.3.7 General Reaction for Thermal Thiol-Ene Click Reaction with PIP-*g*-SiO_2

In a typical reaction, PIP-*g*-SiO_2 (100 mg, 1.21 mmol), azobisisobutyronitrile, or AIBN (99 mg, 0.605 mmol), and propanethiol (0.5 mL, 6.05 mmol) were added to a 20 mL septum-capped vial and dissolved in dry benzene (5.0 mL). The solution was degassed by bubbling argon for 15 minutes. The vial was then placed in an oil bath heated to 80 °C for three hours. A white/yellow material was observed with a fibrous appearance and rubber-like consistency. The polymer was collected with the addition of methanol followed by centrifugation at 6,500 rpm for five minutes. The supernatant was decanted and the solid was dried overnight.

4.4 Results and Discussion

In this work, we present an approach for ethylene/propylene copolymers with high ethylene content grafted to silica nanoparticles with independent

control over polymer composition and molecular weight (Scheme 4.1). To begin, silica nanoparticles were functionalized with an aminosilane reagent followed by an alkylsilane reagent to cap any unreacted silanol groups on the particle surface. The amine-functionalized nanoparticles were then reacted with an activated RAFT agent, DoPAT, to attach RAFT agents directly onto the surface. RAFT activation requires a DCC coupling reaction to promote reactivity of the carbonyl carbon over reaction with the trithioester. To effectively incorporate high ethylene content, a commercially available reagent of 1,3-butadiene dissolved in toluene was used. Isoprene was used over DMB as the propylene source since polyisoprene can undergo a higher degree of hydrogenation due to less constraints over steric hindrance. Additionally, inclusion of DMB would inevitably invoke head-to-head propylene units; using isoprene mitigates this occurrence. Once copolymerized, the polymer-grafted nanoparticles were isolated and subjected to hydrogenation using para-toluenesulfonyl hydrazide (TSH) to convert the unsaturated copolymer into the desired ethylene/propylene copolymer grafted nanoparticles. A set of samples were prepared through this approach. Characterization data is shown in Table 4.1.

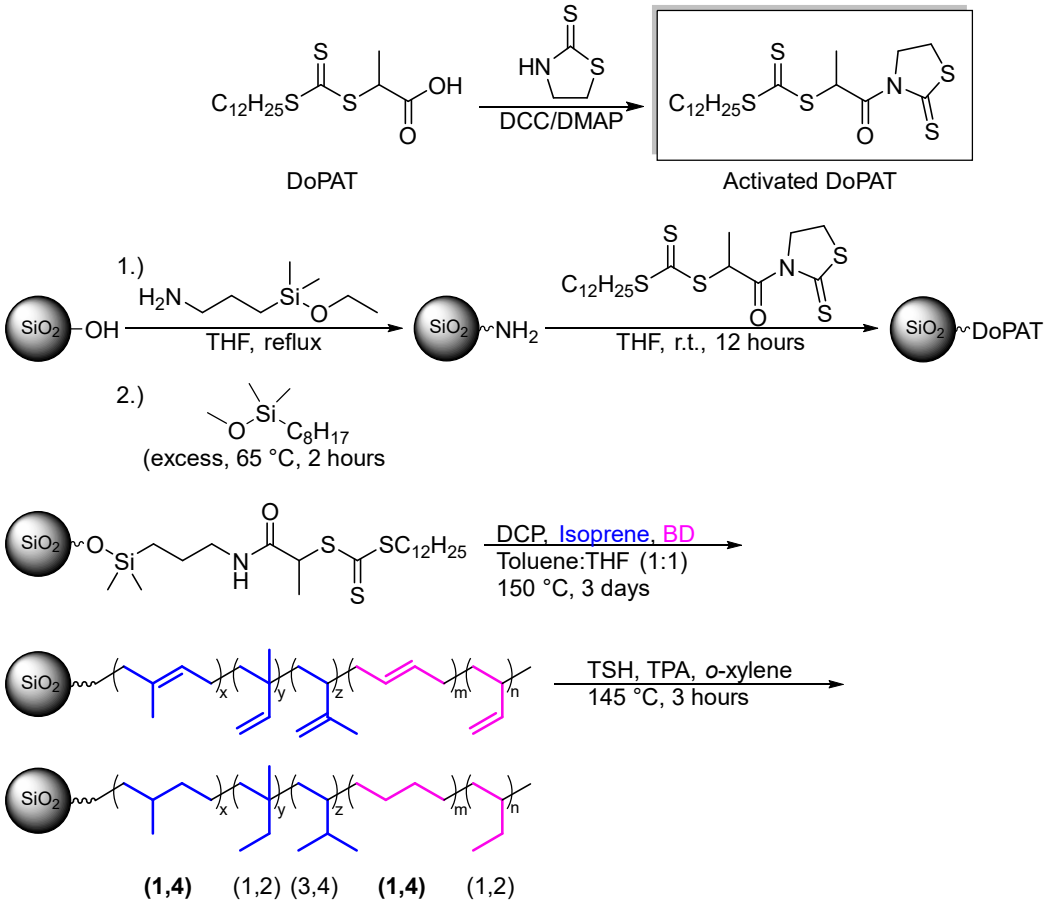

Scheme 4.1: Synthetic approach toward ethylene/propylene copolymers with high ethylene content grafted to silica nanoparticles

Table 4.1: Reaction conditions and results of isoprene and BD copolymerization

Entry[a]	Molecular Weight (kDa)[b]	Isoprene Percentage[c]	T_g (°C)[d]	Thermal Stability (°C)[e]
1	23.2	20/25	-71.5	335
2	22.9	40/48	-65.7	324
3	27.8	60/66	-63.0	308
4	45.6	80/84	-58.1	312
5[f]	40.6	100/-	-64.6	316
6[g]	27.7	0/-	-76.0	319

Polymerizations were all performed at a ratio [Monomer]:[CTA]:[Initiator] of 2,500:1.0:0.15. Reactions were run at 150 °C for three days on nanoparticles with graft density of 0.368 chains/nm^2.[b]Molecular weight was determined via TGA. [c]Isoprene percentage in BD was expressed as theoretical/experimental where experimental was determined via ^{1}H NMR. [d]Glass transition temperature (DSC). [e]Determined via TGA by recording onset of curve from organic mass weight loss. [f]Homopolymer, PIP-*g*-SiO_2. [g]Homopolymer, PBD-*g*-SiO_2.

Copolymerization of isoprene and BD to yield an ethylene/propylene unsaturated precursor is advantageous as it gives a platform for facile determination of polymer composition using common techniques such as ^{1}H NMR. After hydrogenation, the similar chemical environment of protons present would make discerning between the two unmanageable. Additionally, polyethylene and polypropylene are both known for having poor solubility, requiring the use of harsh organic solvents at high temperatures. The isoprene/BD copolymer, however, is readily soluble in common solvents allowing for more

thorough characterization of the grafted polymers prior to hydrogenation. As expected with copolymerization, T_g decreased with increasing amount of BD relative to isoprene. Using the experimental data from homopolymers, PBD-*g*-SiO_2 and PIP-*g*-SiO_2, T_g's calculated using Fox Equation agree well with experimental findings, e.g., Entry 1 and 2 calculated/experimental T_g's are -73/-72 °C and -71/-66 °C, respectively.

To determine compatibility of the two monomers, isoprene and BD, a set of copolymerization reactions were performed with varying amounts of each monomer (Figure 4.1). ^{1}H NMR was used to track the monomer composition in the polymer chain. Due to the methyl group of isoprene, a significant chemical shift between the vinyl protons of the repeating units was observed, resulting in a clear distinction between the two peaks. As the %feed of isoprene decreased, intensity corresponding to the vinyl proton (orange) decreased relative to the other peaks. By normalizing this peak to 1.0 and comparing it to the vinyl proton of BD (blue), a ratio of isoprene and BD repeating units in the spectra could be determined using the equation shown (Figure 4.1b).

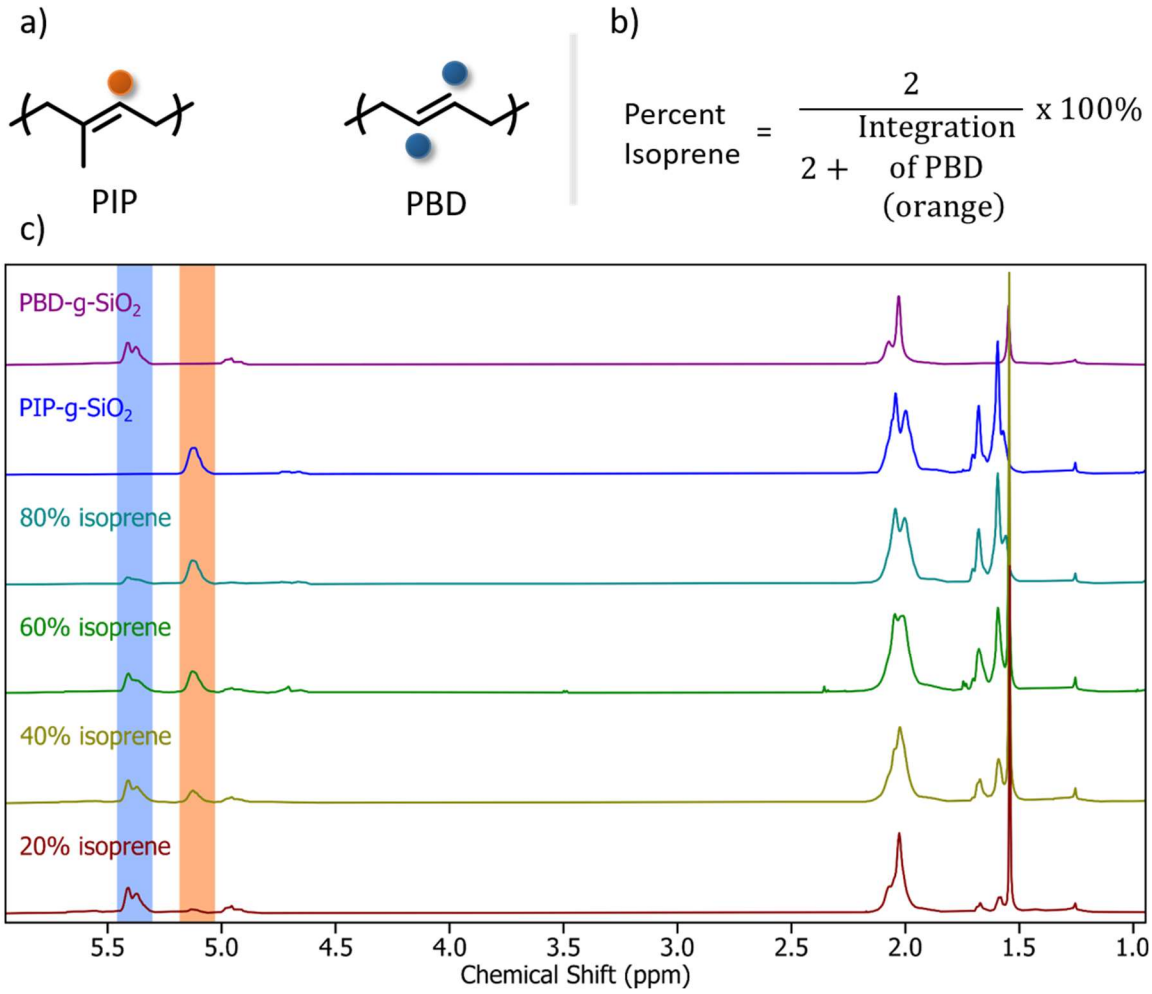

Figure 4.1: (a) Repeating units of PIP (left) and PBD (right), (b) Formula for percent isoprene calculation where integration value for vinyl proton is normalized to 1.0, (c) Stacked ^{1}H NMR spectra from the copolymerization of isoprene and BD with vinyl protons highlighted accordingly for PBD (blue) and PIP (orange).

Hydrogenation conditions were performed on a set of polymer-grafted nanoparticles, and thermal analysis was conducted on the unsaturated copolymers and reduced products (Table 4.2). Using TSH as a hydrogen source can potentially cleave polymer chains from the particle surface since toluenesulfonyl anions have been known to attack siloxane bonds (Si – O – C).[29]

However, this cleavage can be mitigated by having higher grafting density. As seen in Figure 4.2, hydrogenation on the grafted particles with grafting density 0.368 chains/nm^2 results in TGA curves comparable to the unsaturated precursor, indicating grafted polymer chains were retained. A slight increase of polymer mass was expected from the added hydrogens across the double bonds. The onset for polymer combustion increased by approximately 20 °C, signifying thermal stability was improved by the reduction of double bonds. Changes in T_g after hydrogenation were more pronounced in lower isoprene content. This was anticipated as BD repeating units can undergo complete hydrogenation under the current conditions, unlike isoprene repeating units.[30] Lack of melting behavior was observed, likely caused by having three different repeating units present on the copolymer: hydrogenated BD, hydrogenated isoprene, and unsaturated isoprene. For the most part, degree of hydrogenation was able to reach at least 70%, with the exception of Entry 4. This is likely due to the higher molecular weight relative to other entries and high graft density. Based on our earlier results, a dense brush was likely present, therefore limiting reduction from occurring closer to the silica core.

Table 4.2: Characterization of hydrogenated copolymers

Entry	Isoprene Percentage[a]	T_g (°C)[b]	Thermal Stability (°C)[c]	Char Yield (%)[d]	Degree of Hydrogenation (%)[e]
1	20/25	-71.5/ -51.7	335/ 358	29/ 29	93
2	40/48	-65.7/ -63.9	324/ 352	28/ 17	87
3	60/66	-63.0/ -63.0	308/ 347	14/ 21	72
4	80/84	-58.1/ -61.7	312/ 341	16/ 28	37
5	100/-	-64.6/ -56.7	316/ 298	24/ 31	75
6	0/-	-76.0/ -[f]	319/ 383	18/ 22	100

[a]Isoprene percentage in BD was expressed as theoretical/experimental where experimental was determined via ^{1}H NMR. [b]Glass transition temperature (DSC) expressed as before/after hydrogenation. [c]Expressed as before/after hydrogenation. [d]Determined via TGA by recording end of complete combustion of polymer mass. [e]Determined via ^{1}H NMR (^{1}H NMR shown in Figure A.5). [f]After hydrogenation, no T_g feature was observed.

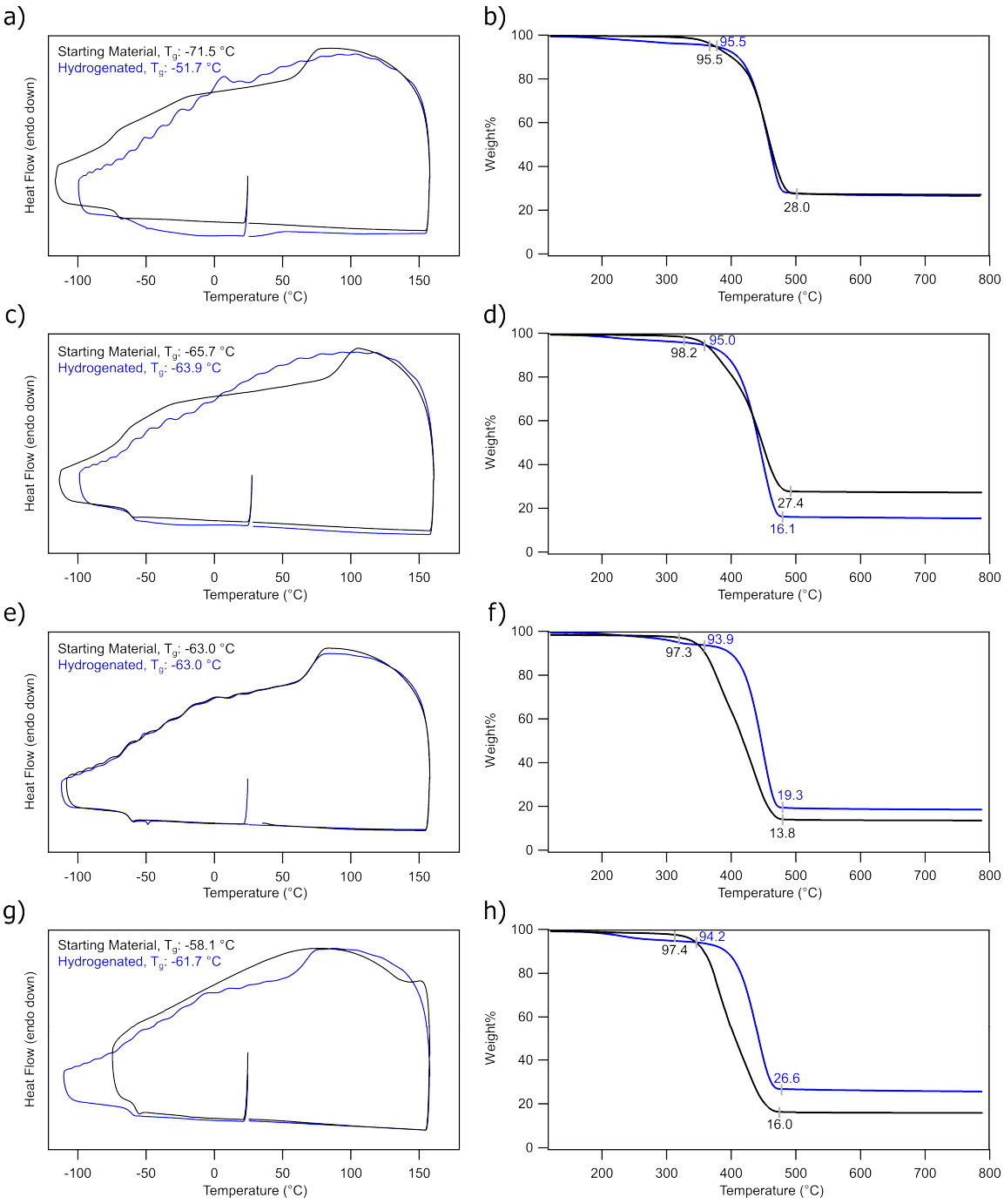

Figure 4.2: Thermal Analysis of polymer nanocomposites with graft density 0.368 chains/nm^2. DSC (left) and TGA (right) were performed before (black) and after hydrogenation (blue). MW of the samples are (Entry 1, a and b) 23.2 kDa, (Entry 2, c and d) 22.9 kDa, (Entry 3, e and f) 27.8 kDa, (Entry 4, g and h) 45.6 kDa.

An issue seen with incorporation of propylene units through addition of isoprene or DMB is partial hydrogenation. Due to the steric constraints, complete hydrogenation was not observed through the traditional approaches using additional TSH equivalence or extended reaction times. With these systems, reactive double bonds left in the system could inevitably oxidize or undergo other reactions, thereby impacting current properties of the material. Conversion of the double bonds could prove to be an effective method for mitigating this concern. Thiol-ene click chemistry is known for its ease of use and near complete conversion in polymeric systems.[31, 32] Thiol-ene click chemistry on PIP-g-SiO_2 with propanethiol was performed as a proof of concept for this approach. Qualitatively, the physical appearance changed drastically, going from a sticky, gel to a soft, spongey-like consistency. Thermal analysis and spectroscopy characterization was also performed (Figure 4.3). DSC shows an increase in T_g of over 20 °C due to the increased branching off the polymer chain. FTIR was indicative the reaction was successful based on disappearance of the stretching frequency corresponding to the C = C – H bond, and ^{1}H NMR supports the claim as the signal of the vinyl proton of the isoprene unit disappeared while peaks from the propyl group were present. TGA also shows an increase in molecular weight, a result from the addition of the propylsulfide group.

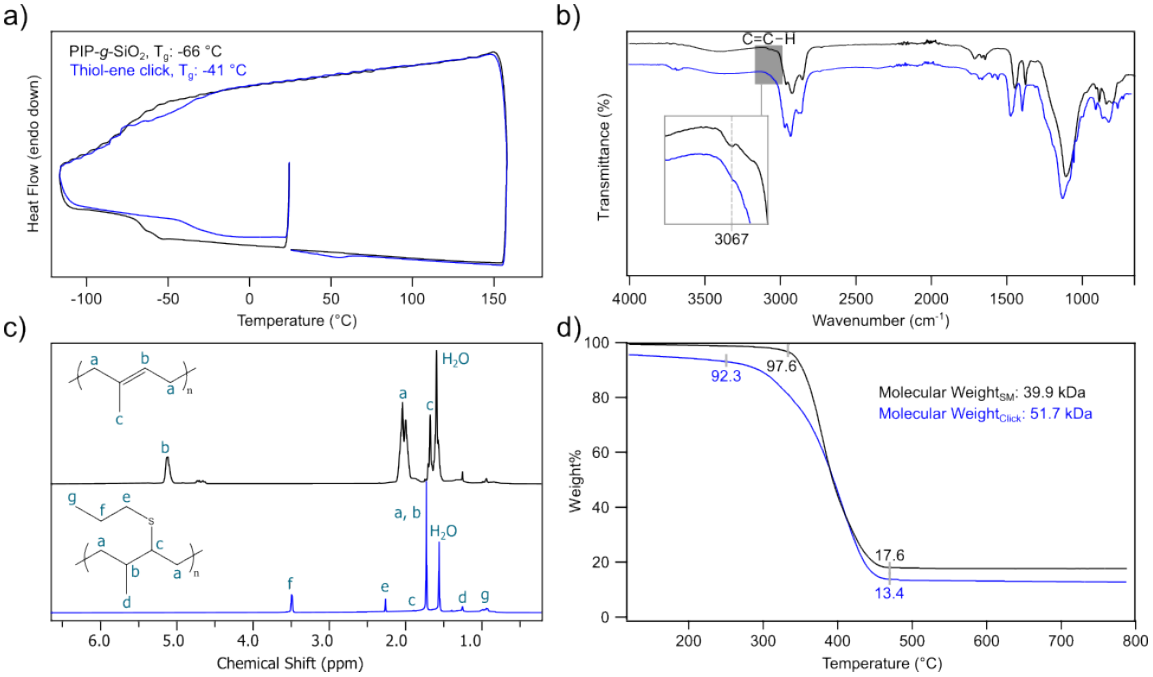

Figure 4.3: Characterization of PIP-g-SiO_2 (black) and product of thiol-ene click reaction with propanethiol (blue): (a) DSC curve; (b) FTIR highlighting disappearance of stretch corresponding to C=C-H stretch; (c) stacked ^1H NMR; (d) TGA showing increase in molecular weight from addition of propane thiol group.

4.5 Conclusions

In this work, a novel approach for an ethylene- and propylene-free synthesis of ethylene/propylene copolymers grafted to silica nanoparticles with high ethylene content was developed along with detailed characterization of the resulting polymers on silica nanoparticles. Utilizing SI-RAFT, controlled polymerization of isoprene and BD onto the nanoparticle surface was achieved and predictable molecular weight was observed. Additionally, the unsaturated isoprene/BD copolymer offered a material with high solubility and ease of

characterization of the polymer composition due to the differences in chemical environments of protons corresponding to the isoprene and BD units.

Using the isoprene/BD as the unsaturated precursors led to ethylene/propylene copolymers with high degree of hydrogenation, and materials with low T_g's. Predictable reactivity of isoprene in BD was observed and, as a result, controlled ratio of ethylene in propylene units was achieved. Although complete hydrogenation could not be achieved with methyl side group-containing copolymers, thiol-ene click reactions using a simple propanethiol reagent demonstrated that the remaining double bonds could be completely eliminated from the copolymers. Such highly branched polyolefins could be useful in some applications as new materials or compatibilizing agents. Development of this synthetic strategy toward olefin-based polymer nanocomposites is a great addition to a polymer chemist's synthetic toolbox as it demonstrates impressive control toward ethylene/propylene copolymers with high ethylene content, predictable molecular weight, and independent control over polymer composition and graft density.

4.6 References

1. Tullo, A. H. Plastic Has a Problem; Is Chemical Recycling the Solution? *Chem. Eng. News*, **2019**, *97*(39).

2. Malpass, D. B.; Band, E. I. "Introduction to Polymers of Propylene" in *Introduction to Industrial Polypropylene*: *Properties, Catalysis, Processes.* (Scrivener, 2012). Pp 1-18.

3. Zhu, J.; Watson, E. W.; Tang, J.; Chen, E. Y.-X. A Synthetic Polymer System with Repeatable Chemical Stability. *Science* **2018**, *360*(6387), 398-403.

4. Ghosh, K.; Jones, B. H. Roadmap to Biodegradable Plastics – Current State and Research Needs. *ACS Sustainable Chem. Eng.* **2021**, *9*(18) 6170-6187.

5. Haider, T.; Shyshov, O.; Suraeva, O.; Lieberwirth, I.; Delius, M. v.; Wurn, F. R. Long-chain Polyorthoesters as Degradable Polyethylene Mimics. *Macromolecules* **2019**, *52*(6), 2411-2420.

6. Ma, Y.; Zhou, H.; Jiang, X.; Polaczyk, P.; Xiao, R.; Zhang, M.; Huang, B. The Utilization of Waste Plastics in Asphalt Pavements: A review. *Elsevier* **2021**, *2*(15).

7. Teh, J. W.; Rudin, A.; Keung J. C. A Review of Polyethylene-propylene Blends and Their Compatibilization. *Advances in Polymer Technology* **1994**, *13*(1), 1-23.

8. Xanthos, M. Recycling of the #5 Polymer. *Science*, **2012**, *337*, 700-702.

9. Aumnate, C.; Rudolph, N.; Sarmadi, M. Recycling of Polypropylene/Polyethylene Blends: Effect of Chain Structure on the Crystallization Behaviors. **2019**, *11*.

10. Lin, Y.; Yakovleva, V.; Chen, H.; Hiltner, A.; Baer, E. Comparison of Olefin Copolymers as Compatibilizers for Polypropylene and High-density Polyethylene. *J. Appl. Polym. Sci.* **2009**, *113*, 1945-1952.

11. Colbeaux, A.; Fenouillot, F.; Gerard, J.-F.; Taha, M.; Wautier, H. Compatibilization of a Polyolefin Blend through Covalent and Ionic Coupling of Grafted Polypropylene and Polyethylene. I Rheological, Thermal, and Mechanical Properties. *J. Appl. Polym. Sci.* **2005**, *95*, 312-320.

12. Xanthos, M.; Dagli, S. S.; Compatibilization of Polymer Blends by Reactive Processing. *Polym. Eng. Sci.* **1991**, *31*, 929-935.

13. Tselios, C.; Bikiaris, D.; Maslis, V.; Panayiotou, C.; In Situ Compatibilization of Polypropylene-Polyethylene Blends: A Thermomechanical and Spectroscopic Study. *Polymer*, **1998**, *39*, 6807-6817.

14. Chiu, W.-Y.-; Fang, S. –J.Mechanical Properties and Morphology of Crosslinked PP/PE Blends and PP/PE/Propylene-Ethylene Copolymer Blends. *J. Appl. Polym. Sci.* **1985**, *30*, 1473-1489.

15. Xu, J.; Eagen, J. M.; Kim, S.- S.; Pan, S.; Lee, B.; Klimovica, K.; Jin, K.; Lin, T.-W.; Howard, M. J.; Ellison, C. J.; LaPointe, A. M.; Coates, G. W.; Bates, F. S. Compatibilization of Isotactic Polypropylene (*i*PP) and High-Density Polyethylene (HDPE) with *i*PP-PE Multiblock Copolymers. *Macromolecules* **2018**, *51*, 8585-8596.

16. Eagen, J. M.; Xu, J.; Girolamo, R. D.; Thurber, C. M.; Macosko, C. W.; LaPointe, A. M.; Bates, F. S.; Coates, G. W. Combining Polyethylene and Polypropylene: Enhanced Performance with PE/*i*PP Multiblock Polymers. *Science* **2017**, *355*, 814-816.

17. Klimovica, K.; Pan, S.; Lin, T.- W.; Peng, X.; Ellison, C. J.; LaPointe, A. M.; Bates, F. S.; Coats, G. W. Compatibilization of *i*PP/HDPE Blends with PE-*g*-*i*PP Graft Copolymers. *ACS Macro. Lett.* **2020**, *9*, 1161-1166.

18. Wang, H.; Onbulak, S.; Weigand, S.; Bates, F. S.; Hillmyer, M. A. Polyolefin Graft Copolymers Through a Ring-opening Metathesis Grafting Through Approach. *Polym. Chem.* **2021**, *12*, 2075-2083.

19. Arriola, D. J.; Carnahan, E. M.; Hustad, P. D.; Kuhlman, R. L.; Wenzel, T. T. Catalytic Production of Olefin Block Copolymers Via Chain Shuttling Polymerization. *Science* **2006**, *312*, 714-719.

20. Lopez-Barron, C. R.; Tsou, A. H. Strain Hardening of Polyethylene/Polypropylene Blends Via Interfacial Reinforcement with Poly(Ethylene-cb-Propylene) Comb Block Copolymers. *Macromolecules* **2017**, *50*, 2986-1995.

21. Tsou, A. H.; Lopez-Barron, C. R.; Jiang, P.; Crowther, D. J.; Zeng, Y. Bimodal Poly(Ethylene-cb-Propylene) Comb Block Copolymers from Serial Reactors: Synthesis and Applications as Processability Additives and Blend Compatibilizers. *Polymer* **2016**, *104*, 72-82.

22. Antunes, M.; Realinho, V.; Ardanuy, M.; Mopoch, M. L.; Velasco, J. I. Mechanical Properties and Morphology of Multifunctional Polypropylene Wastes. *Cell. Polym.* **2011**, *30*(4), 187-200.

23. Naushad, M.; Nayak, S. K. Mohanty, S.; Kalita, H.; Panda, B. P. Damage Tolerance Behavior of Cloisite 15A Incorporated Recycled Polypropylene Nanocomposites and Bionanocomposites. *J. Exp. Nanosci.* **2016**, *11*(14), 1110-1126.

24. Zdiri, K.; Elamri, A.; Hamdaoui, M.; Harzallah, O.; Khenoussi, N.; Brendle, J. Reinforcement of Recycled PP Polymers by Nanoparticles Incorporation. *Green Chemistry Letters and Reviews* **2018**, *11*(3), 296-311.

25. Garofalo, E.; Maio, L. D.; Scarfato, P.; Apicella, A.; Protopapa, A.;Incarnato, L. Nanosilicates in Compatibilized Mixed Recycled Polyolefins: Rheological Behavior and Film Production in a Circular Approach. *Nanomaterials* **2021**, *11*, 1-19.

26. Bansal, A.; Yang, H.; Benicewicz, B. C.; Kumar, S. K.; Schadler, L. S. Controlling the Thermomechanical Properties of Polymer Nanocomposites by Tailoring the Polymer-particle Interface. *J. of Polym. Sci.: Part B: Polym. Phys.* **2006**, *44*(20), 2944-2950.

27. Mackay, M. E.; Tuteja, A.; Duxbury, P. M.; Hawker, C. J.; Horn, B. V.; Guan, Z.; Chen, G.; Krishnan, R. S. General Strategies for Nanoparticle Dispersion. *Science* 2006, *311*, 1740-1743.

28. Hore, M. J. A.; Korley, L. T. J.; Kumar, S. K. Polymer-Grafted Nanoparticles. *J. Appl. Phys.* **2020**, *128*, 030401.

29. Petzetakis, N.; Stone, G. M.; Balsara, N. P. Synthesis of Well-Defined Polyethylene-Polydimethylsiloxane-Polyethylene Triblock Copolymers by Diimide-Based Hydrogenation of Polybutadiene Blocks. *Macromolecules* **2014**, *14*(13), 4151-4159.

30. Hahn. S. F. An Improved Method for the Diimide Hydrogenation of Butadiene and Isoprene Containing Polymers. *J. of Polym. Sci.: Part A: Polym. Chem.* **1992**, *30*, 397-408.

31. Lowe, A. B. Thiol-ene "Click" Reactions and Recent Applications in Polymer and Materials Synthesis. *Polym. Chem.* **2010**, *1*, 17-36.

32. Hoyle, C. E.; Bowman, C. N. Thiol-Ene Click Chemistry. *Angew. Chem. Int. Ed.* **2010**, *49*, 1540-1573.

CHAPTER 5

SUMMARY AND OUTLOOK

5.1 Summary

The work discussed in this dissertation paves a foundation for polyolefin nanocomposites, which would otherwise be challenging to produce through methods found in literature examples due to synthetic barriers, e.g., solubility resulting in low polymer molecular weight and characterization limitations, restrictive copolymer architecture, and lack of approaches for grafting onto nanoparticles. In this work, SI-RAFT polymerization was used to promote synthesis and grow chains directly onto the nanoparticle surface. Nanoparticles functionalized with RAFT agents also provided a "target" to be quantified for graft density determination prior to polymerization, a benefit absent in other surface-initiated polymerization techniques. Quantifying graft density prior to polymerization is advantageous as it offers an alternative method for polymer molecular weight determination by using the polymer to silica mass ratio. In each chapter, polymerization of butadiene-based monomers yielded soluble materials, which allowed for higher molecular weight to be achieved. Majority of synthetic approaches for polyolefin materials directly synthesize the saturated polymer and, as a result, limit copolymer architecture to blocks, or branches built from macromonomers since the only approach to effectively quantify the ethylene to propylene ratio is by measuring increase in molecular weight after each reaction.

In this work, random copolymers were synthesized and the ethylene to propylene ratio was determined accurately with solution-based characterization.

Chapter 2 discusses an approach toward ethylene/propylene-like copolymers with high propylene content grafted to silica nanoparticles. Copolymerization of isoprene and DMB yielded an unsaturated precursor of an ethylene/propylene copolymer that was used to characterize the polymer composition through solution-based characterization (i.e., ^{1}H NMR). RAFT polymerization of the diene monomers resulted in a polymer with predictable ethylene and propylene content, and hydrogenation of the unsaturated copolymers led to polymers with ethylene/propylene content with low T_g's and head-to-head propylene isomeric structure. Thermal analysis studies demonstrated how molecular weight effected the results of the hydrogenation conditions with grafted polymers. Due to the steric hindrance of the DMB and isoprene repeating units, only partial hydrogenation was achieved.

In chapter 3, a new ethylene-free approach for polyethylene-grafted silica nanoparticles was discussed. RAFT polymerization of 1,3-butadiene displayed controlled synthesis of the polymer with predictable molecular weight on two sets of nanoparticles with different graft densities. Hydrogenation of the butadiene polymer compared to isoprene and DMB from Chapter 2 produced a completely hydrogenated product, with vastly different DSC curves compared to the

unsaturated precursor, including disappearance of the T_g feature and presence of a distinct crystallization peak. At low graft density, the crystallization peak corresponding to the grafted saturated PBD was not observed due to a significantly lower amount of polymer relative to the silica mass.

Chapter 4 is an extension of the work from Chapter 2 with components from Chapter 3, where ethylene/propylene copolymers grafted to silica nanoparticles were prepared with high ethylene content. Instead of using DMB, copolymerization of 1,3-butadiene and isoprene was performed to give higher range of ethylene in the system than was possible with previous approaches. Additionally, hydrogenation of the copolymers composed of these diene monomers produced a polymer with significantly higher hydrogenation compared to ones with DMB. Obtaining the unsaturated precursor still offered ease of characterizing polymer composition, and control over ethylene/propylene composition was not sacrificed. Instead, the polymers produced closer resembled ethylene/propylene copolymers since head-to-head propylene units were not present, and although complete hydrogenation could not be completed, thiol-ene click reaction with propanethiol was demonstrated to be an effective strategy to fully eliminate any unreacted double bonds. This also provides an additional strategy to increase branching.

5.2 Future Work

With an effective approach toward polyolefin brushes with tunable ratio of ethylene to propylene units paired with independently varied grafting density and polymer molecular weight, extensive studies of polyolefin nanocomposites and their structure-property relationship can be performed.

Firstly, testing the improved mechanical toughness of the material should be performed. This would be done by preparing thin films of both neat polymer and polymer-grafted nanoparticles. Identical molecular weights and polymer composition should be obtained so a more accurate representation of the effect on nanoparticle addition can be observed. After thin films are prepared, "dog bone" shaped materials will be prepared, in triplicates of each sample to remove potential outliers in the results. Tensile testing would then be performed on these samples to observe the tensile strength, maximum elongation, and breaking strength. With the incorporation of nanoparticles, improved tensile stiffness and strength are expected to be observed when compared to the neat polymers. Afterwards, tensile tests would then be performed on copolymer samples of varying isoprene in DMB/BD and their respective hydrogenated products. Due to the larger difference in degree of hydrogenation, it's likely the isoprene in DMB will have similar results to the hydrogenated counterpart, whereas the isoprene in BD and the hydrogenated product will have a more prominent change since

elevated degree of hydrogenation can be achieved. The other variable in optimizing the mechanical properties of the material is the morphology, or the organization of the nanoparticles. Varying graft density and polymer molecular weight in the polymer matrix will achieve various morphologies, each giving different properties. So, the next step would be to explore the changes in morphology, from aggregates and sheets to strings and well-dispersed. These changes in morphology would be observed with SEM imaging.

Reinforcing polymeric materials with nanoparticles is a powerful strategy, and as mentioned previously, morphology of the particles plays large role on the improved properties achieved. Typically, polymer nanocomposites are blended in a polymer matrix of similar chemistry to the grafted polymer. This approach could be applied toward a different application. As mentioned previously, blending polymers notoriously result in phase-separated mixtures due to the immiscible nature of many polymer combinations. To combat this, compatibilizers have been developed with the goal to lower the entropic barrier of mixing immiscible polymers. The PE/PP copolymer-grafted nanoparticles prepared in this work has great potential in compatibilizing the infamous pair immiscible polymers, PE and PP. For this study, PE via RAFT would be blended with commercially available *i*PP at a 70/30 ratio, respectively. To determine the optimal system, a study including several experiments should be conducted. The first study is to find the

prime polymer composition of PE/PP. This would require preparing several samples from 100% to 50% PE in PP using isoprene and BD to achieve higher degree of hydrogenation. After preparing these samples, they would then be annealed for several days, and TEM images would be taken throughout the time to observe any polymer agglomerations.

After determining an effective ratio, the next step would be to tune polymer molecular weight and graft density to adjust the morphology in the system. In homopolymer matrices, dispersion in the polymer matrix is typically sought out; however, in a polymer blend matrix, an effective approach would be to target the weakest point of the material: the interface between the PE and PP matrix. Localizing particles at the interface offers a surfactant-like behavior lowering the interfacial tension between the two polymers while also strengthening those areas. So, for this step, samples of varying graft density and polymer molecular weight using the ratio determined prior would be produced. With these samples, TEM imaging would be performed to observe the organization of particles in the system. Additionally, thin films would be prepared for tensile testing and the results would be compared to observe the difference between dispersed particles in the matrix and those with localized particles at the polymer-polymer interface. The final experiments would then be repeated at varying silica loadings (i.e., 0.5, 1, 2, 3, and 5%. Through the extensive studies, a PP/PE copolymer polymer

nanocomposite could be determined with applications toward improving recycled materials rather than trying to find a cheaper, more environmentally friendly PE.

Preparing materials using the PE prepared via RAFT with BD would be an interesting avenue to explore since it's an extremely low-density form of PE. Compared to the more commercially available HDPE and LDPE, this PE is expected to have even higher flexibility due to the more frequent branching. Like before, preparing films of the PE-*g*-SiO_2 and neat PE via RAFT to run tensile testing would be the start. The other aspect of this material would be to study the semicrystalline nature of the material. This would entail blending PE-*g*-SiO_2 with a PE matrix prepared via RAFT. After annealing the samples, the crystallization front could then be observed using atomic force microscopy. By adjusting the crystallization rate of the polymer, organization through crystallization of the particles could also be studied, whether the particles organize in the interlamellar region or in the amorphous region.

While a small part of this work, combining thiol-ene click chemistry and unsaturated polymers offer a facile and effective approach toward controlled synthesis of LDPE. In this dissertation, addition of thiol groups was utilized primarily to convert all double bonds. With the high efficacy of this reaction in a polymeric system, precision branching can be performed at controlled lengths. This project would be tackled by first synthesizing linear unsaturated chains

through ROMP. By using monomers such as cyclooctene or cyclooctadiene, a double bond can predictably be found at every eight or four carbons. Afterwards, widely commercially available thiol groups could be used for varying chain lengths attached to the backbone. With these variables, a study on the changes in branching frequency and chain length could then be achieved. Increasing either of these variables would likely lower the melting point. Afterwards, crystallization studies could be performed like with the PE via RAFT approach.

In summary, this work displays powerful strategies toward synthesis of various polyolefin nanocomposites that can expanded and tailored toward various applications whether it be in exploratory work with semicrystalline systems using LDPE-like polymers or for a more practical application such as being used as a compatibilizer with surface-like behavior.

APPENDIX A

SUPPLEMENTAL INFORMATION

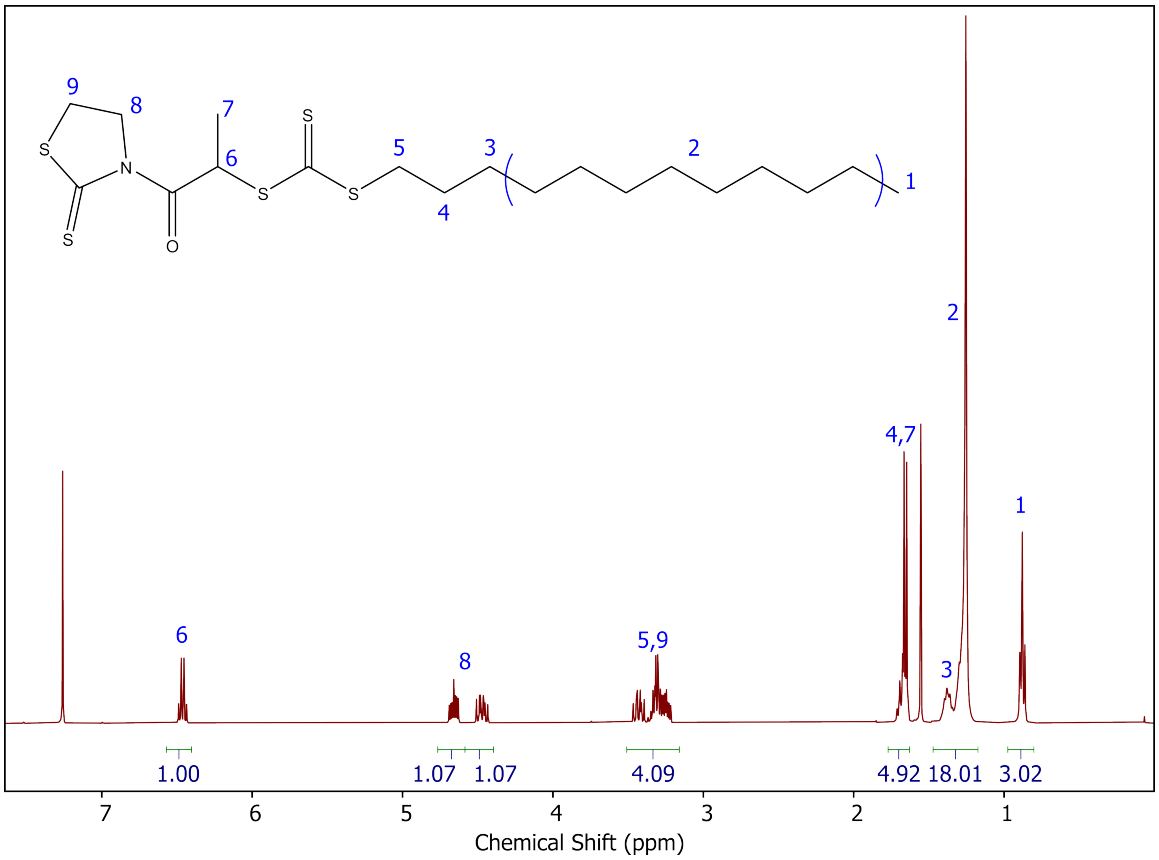

Figure A.1: ^{1}H NMR (300 MHz, $CDCl_3$) spectrum of activated DoPAT

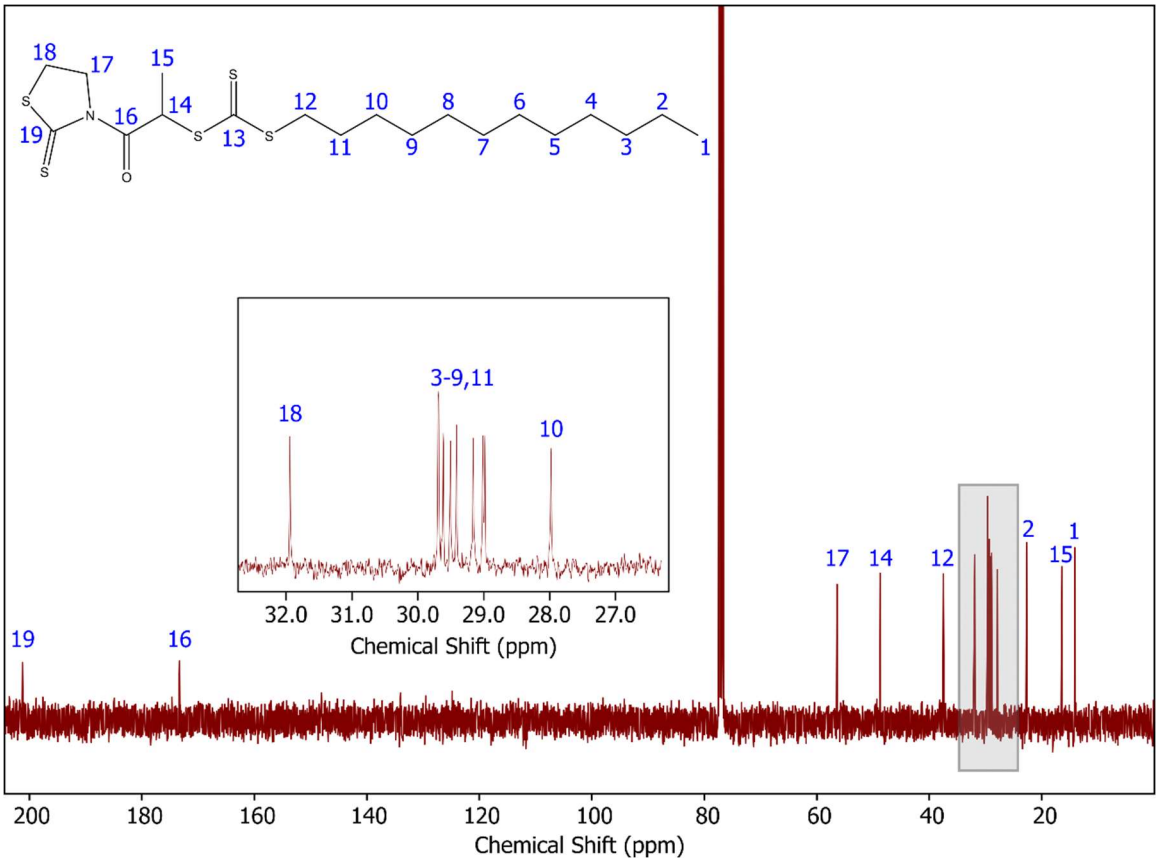

Figure A.2: ^{13}C NMR (300 MHz, $CDCl_3$) spectrum of activated DoPAT

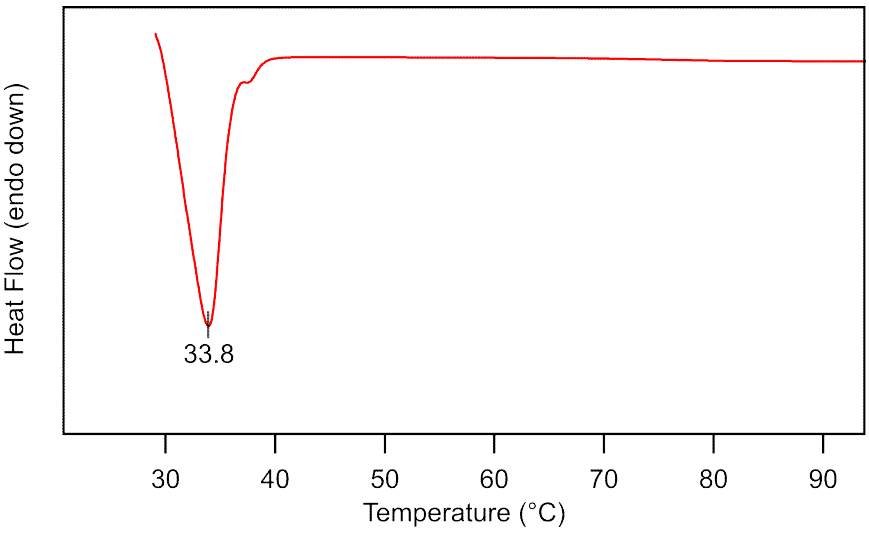

Figure A.3: DSC of activated DoPAT

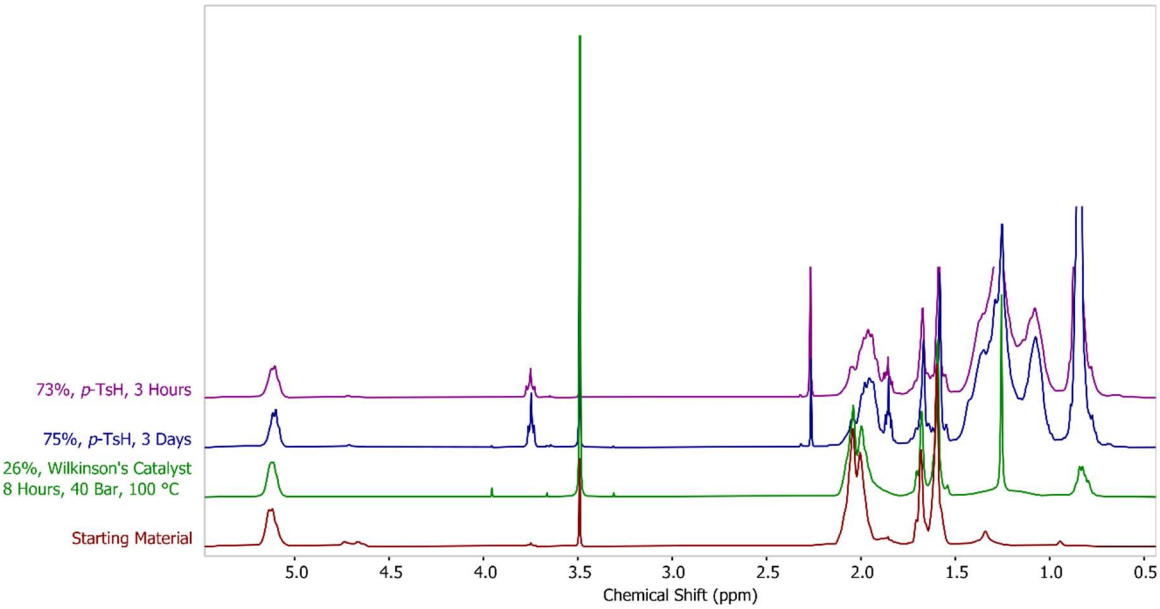

Figure A.4: ^{1}H NMR (300 MHz, $CDCl_3$) stacked spectra comparing result of different hydrogenation conditions with PIP-g-SiO_2

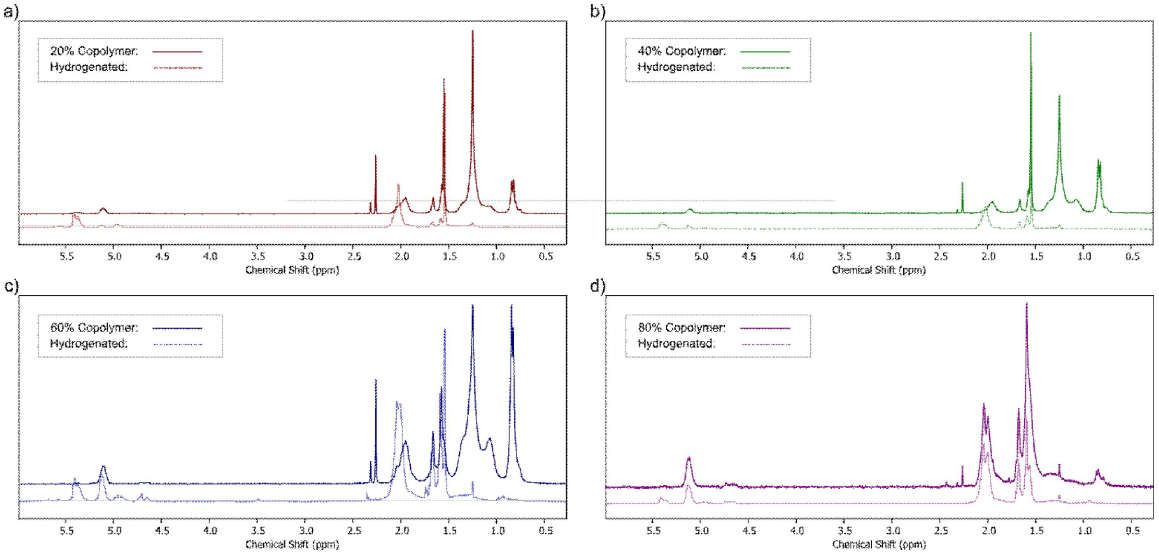

Figure A.5: ^{1}H NMR (300 MHz, $CDCl_3$) stacked spectra of unsaturated copolymers (solid line) and their respective hydrogenated product (dashed line). (a) Entry 1, (b) Entry 2, (c) Entry 3, (d) Entry 4.

APPENDIX B

PERMISSION TO REPRINT

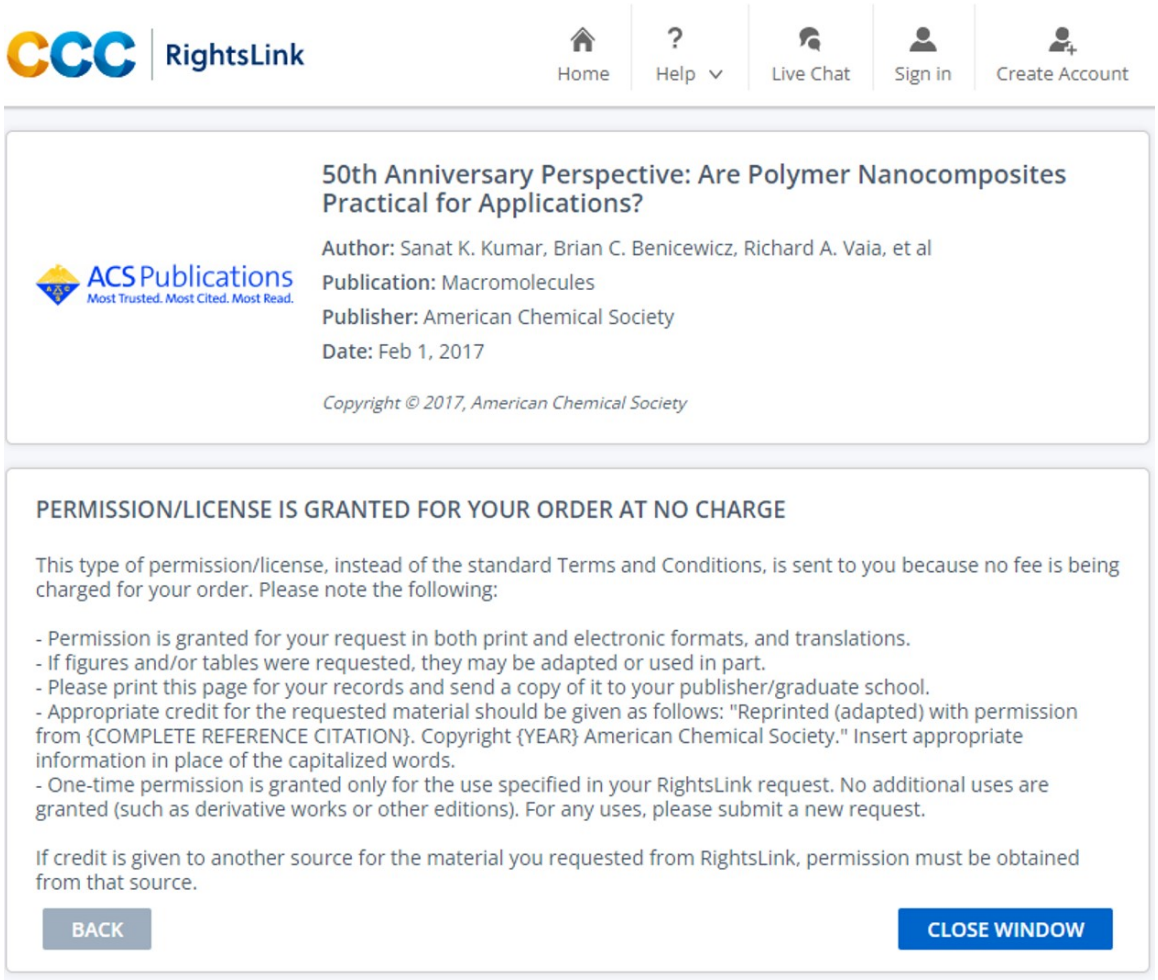

Figure B.1: Permission to reprint Figure 1.3

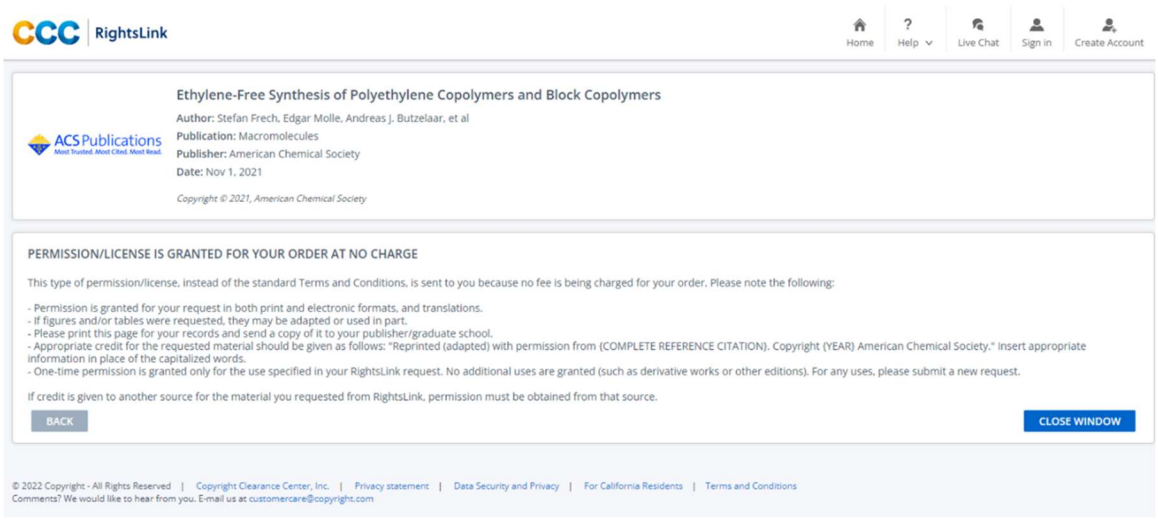

Figure B.2: Permission to reprint Figure 1.7